

# Nuclear interactions and quantum Monte Carlo methods

Maria Piarulli—Washington University, St. Louis

July 11-13, 2022

## Lecture 3: What can we calculate?

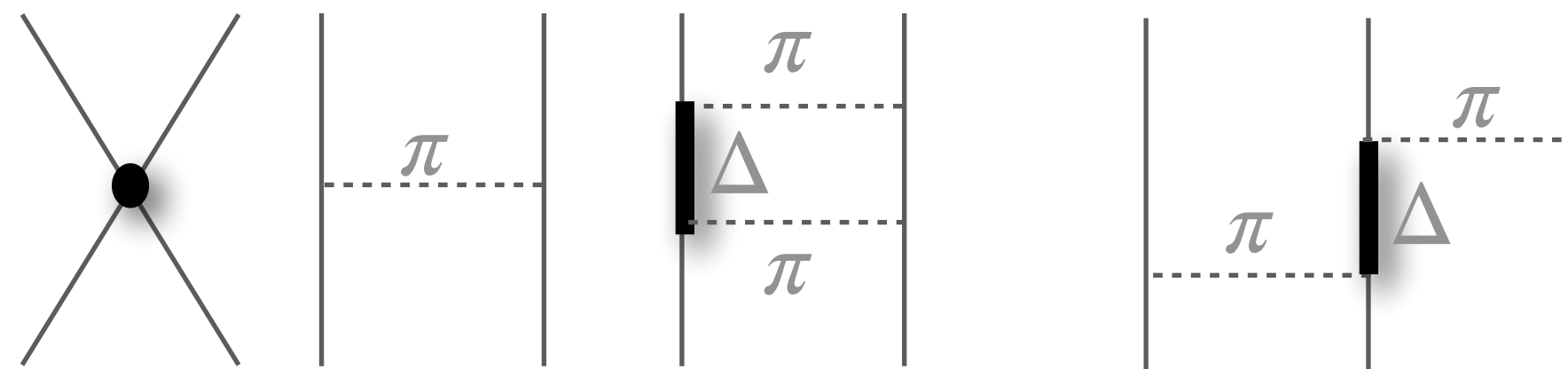
# Many-body Nuclear Interactions

Many-body Nuclear Hamiltonian

$$H = \sum_{i=1}^A \frac{\mathbf{p}_i^2}{2m_i} + \sum_{i<j=1}^A \overbrace{v_{ij}}^{\text{th+exp}} + \sum_{i<j<k=1}^A \overbrace{V_{ijk}}^{\text{th+exp}} + \dots$$

one-body
two-body (NN)
three-body (3N)

- Accurate understanding of the interactions/correlations between nucleons in **pairs**, **triplets**, .. ( $v_{ij}$  and  $V_{ijk}$  are the **two**- and **three**-nucleon forces)
- Operators constrained by experimental data; fitted parameters encode underlying QCD dynamics



long-range  $r \sim m_\pi^{-1}$ : pion-exchange  
 intermediate range  $r \sim (2m_\pi)^{-1}$ : ex. two-pion exchange  
 short-range: ex. contact terms

In our Quantum Monte Carlo calculations we use:

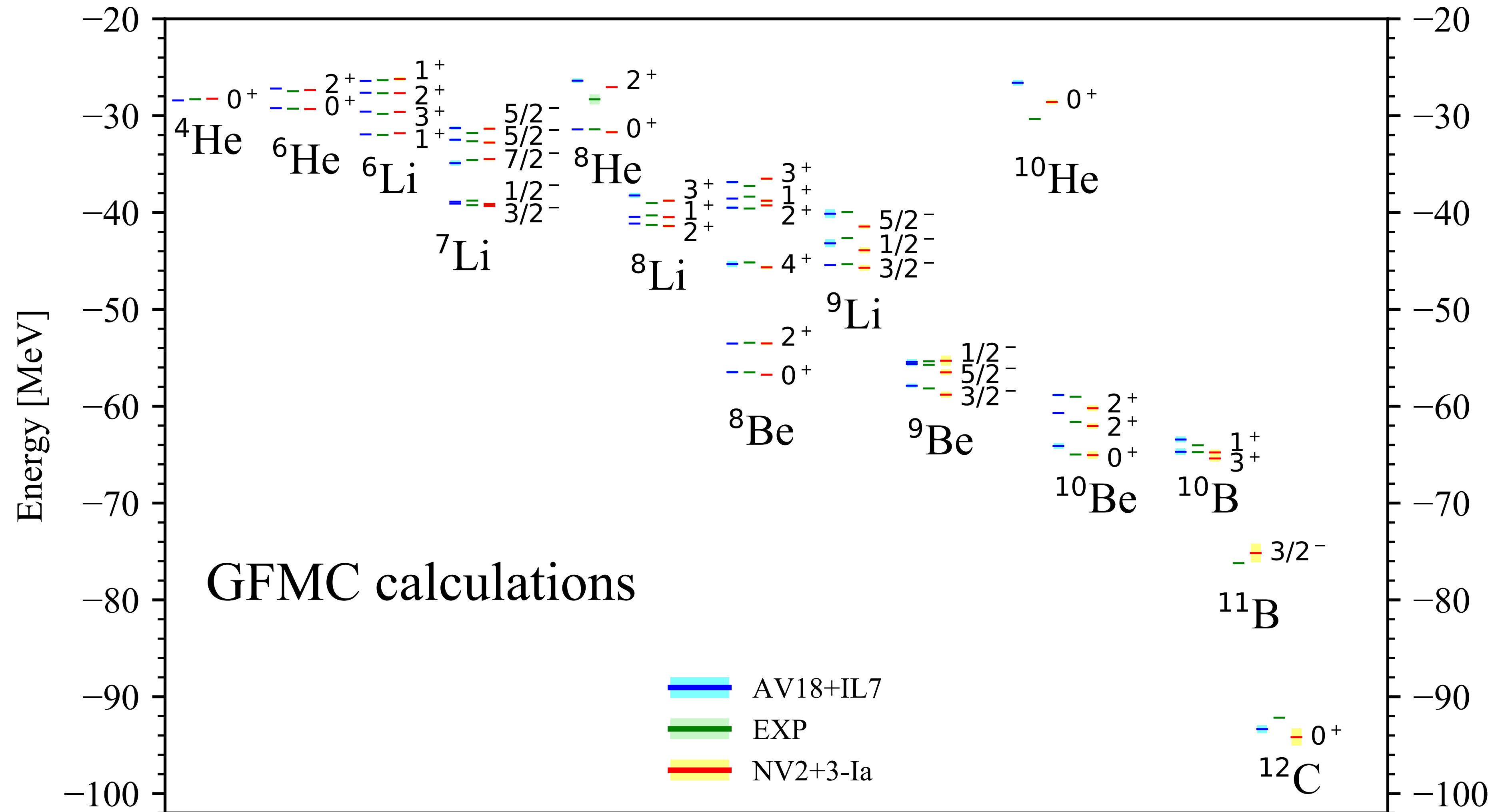
- **AV18+UIX**; **AV18+IL7** phenomenological models

Wiringa, Stoks, Schiavilla PRC **51**, 38 (1995); J. Carlson et al. NP **A401**, 59 (1983); S. Pieper et al. PRC **64**, 014001 (2001)

- chiral  $\pi N \Delta$  **N3LO+N2LO** Norfolk models

MP et al. PRC **91**, 024003 2015; PRC **94**, 054007 2016; MP et al. PRL **120**, 052503 (2018); A. Baroni, MP et al. PRC **98**, 044003 (2018)

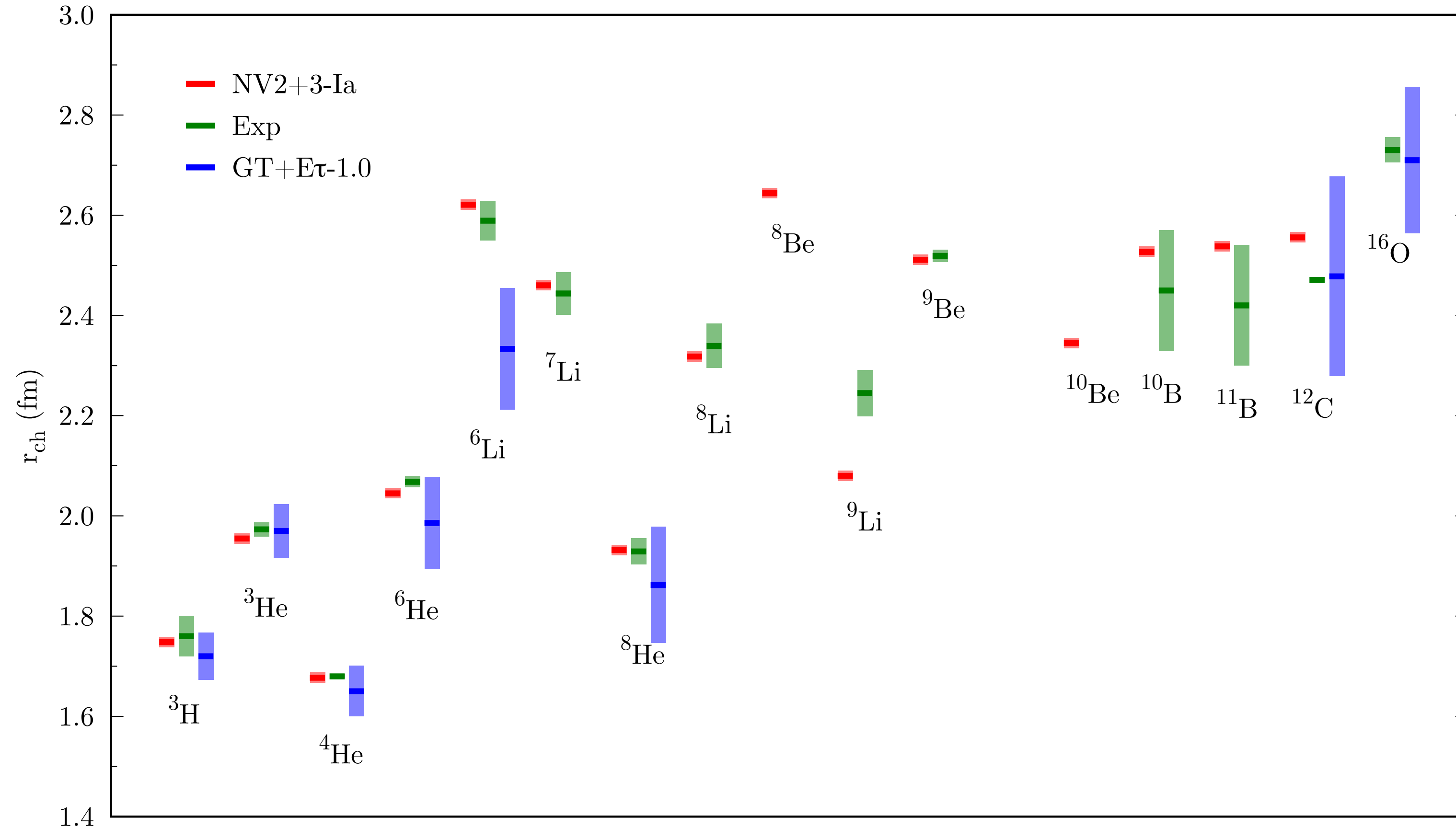
# Binding energies of light nuclei



- Studied 37 different nuclear states in  $A \sim 4 - 12$  nuclei. Comparison between the phenomenological AV18+IL7 model and experiment.
- The agreement with experiment is good for both Hamiltonians: absolute binding energies very close to experiment, and excited states reproducing the observed ordering, indicating reasonable one-body spin orbit splittings.



# Charge radii of light nuclei



- Charge radii with respect to experimental data (GFMC for NV2+3-Ia and AFDMC for GT+Eτ-1.0)
- Overall agreement with the experimental data for both models
- For NV2+3-Ia, <sup>9</sup>Li charge radius underpredicted, <sup>12</sup>C slightly overestimated
- For GT+Eτ-1.0, <sup>6</sup>Li charge radius underpredicted (issue with AFDMC w.f.)

$$\langle r_{\text{ch}}^2 \rangle = \langle r_{\text{pt}}^2 \rangle + \langle R_p^2 \rangle + \frac{A-Z}{Z} \langle R_n^2 \rangle + \frac{3\hbar^2}{4M_p^2 c^2} + \langle r_{\text{so}}^2 \rangle$$

point-nucleon radius

proton radius = 0.770(9) fm<sup>2</sup>

neutron radius = -0.116(2) fm<sup>2</sup>

Darwin-Foldy correction ≈ 0.033 fm<sup>2</sup>

spin-orbit correction

$$\text{point-nucleon radius } \langle r_N^2 \rangle = \frac{1}{\mathcal{N}} \langle \Psi | \sum_i \mathcal{P}_{N_i} |\mathbf{r}_i|^2 | \Psi \rangle$$

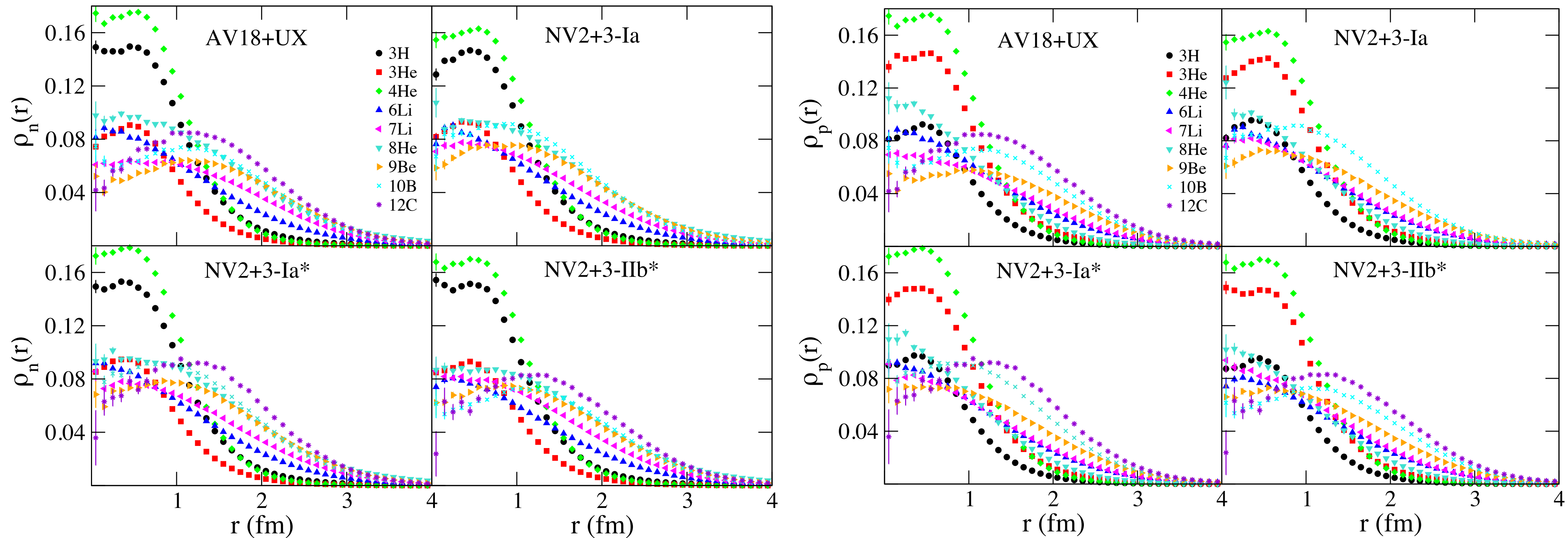
▸  $\mathbf{r}_i$  is the intrinsic nucleon coordinate

▸  $\mathcal{N}$  is the number of protons or neutrons,

$$\text{▸ } \mathcal{P}_{N_i} = \frac{1 \pm \tau_{z_i}}{2}$$

# Single-nucleon densities

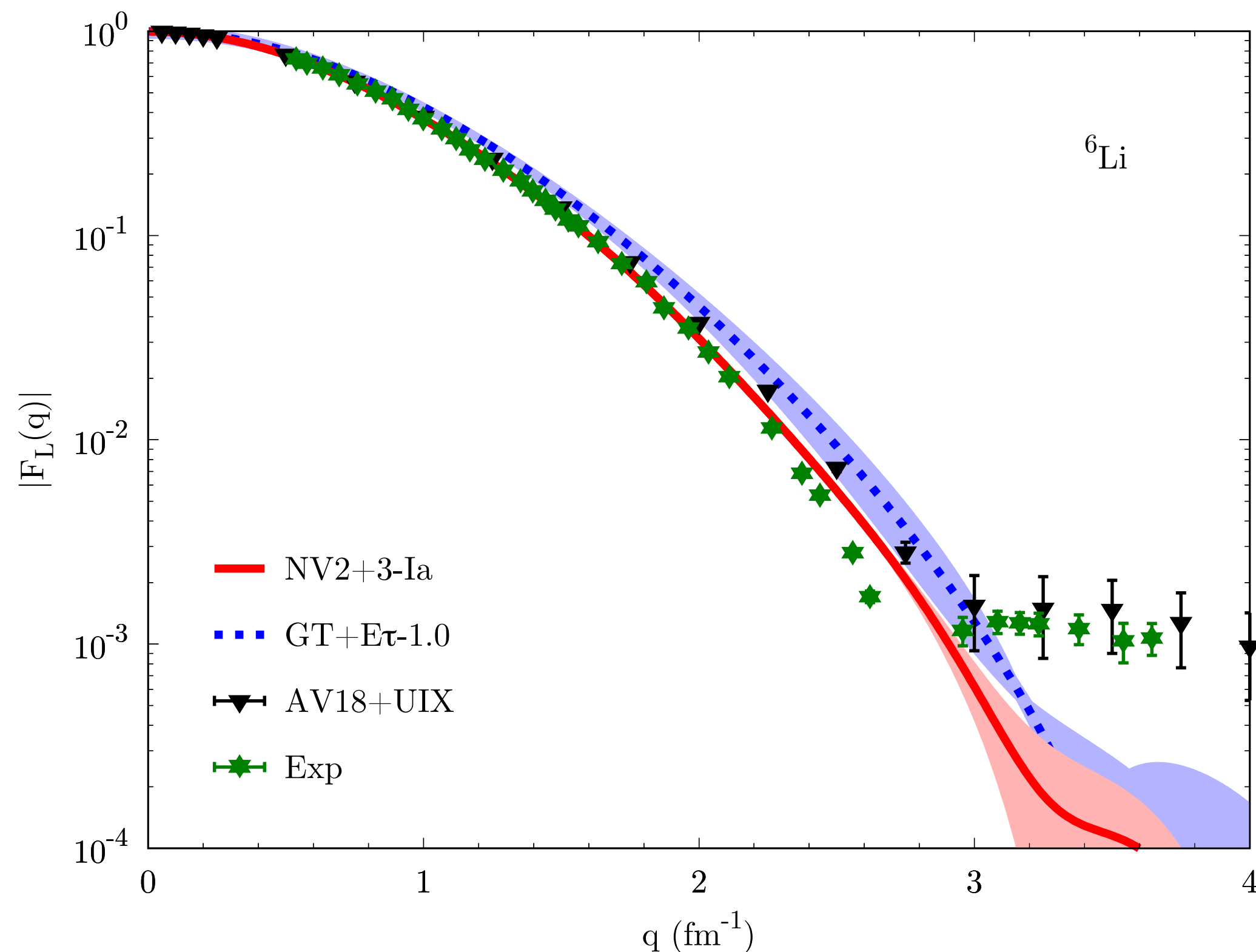
- In QMC methods, single-nucleon densities are calculated as:  $\rho_N(r) = \frac{1}{4\pi r^2} \langle \Psi | \sum_i \mathcal{P}_{N_i} \delta(r - |\mathbf{r}_i - \mathbf{R}_{\text{cm}}|) | \Psi \rangle$



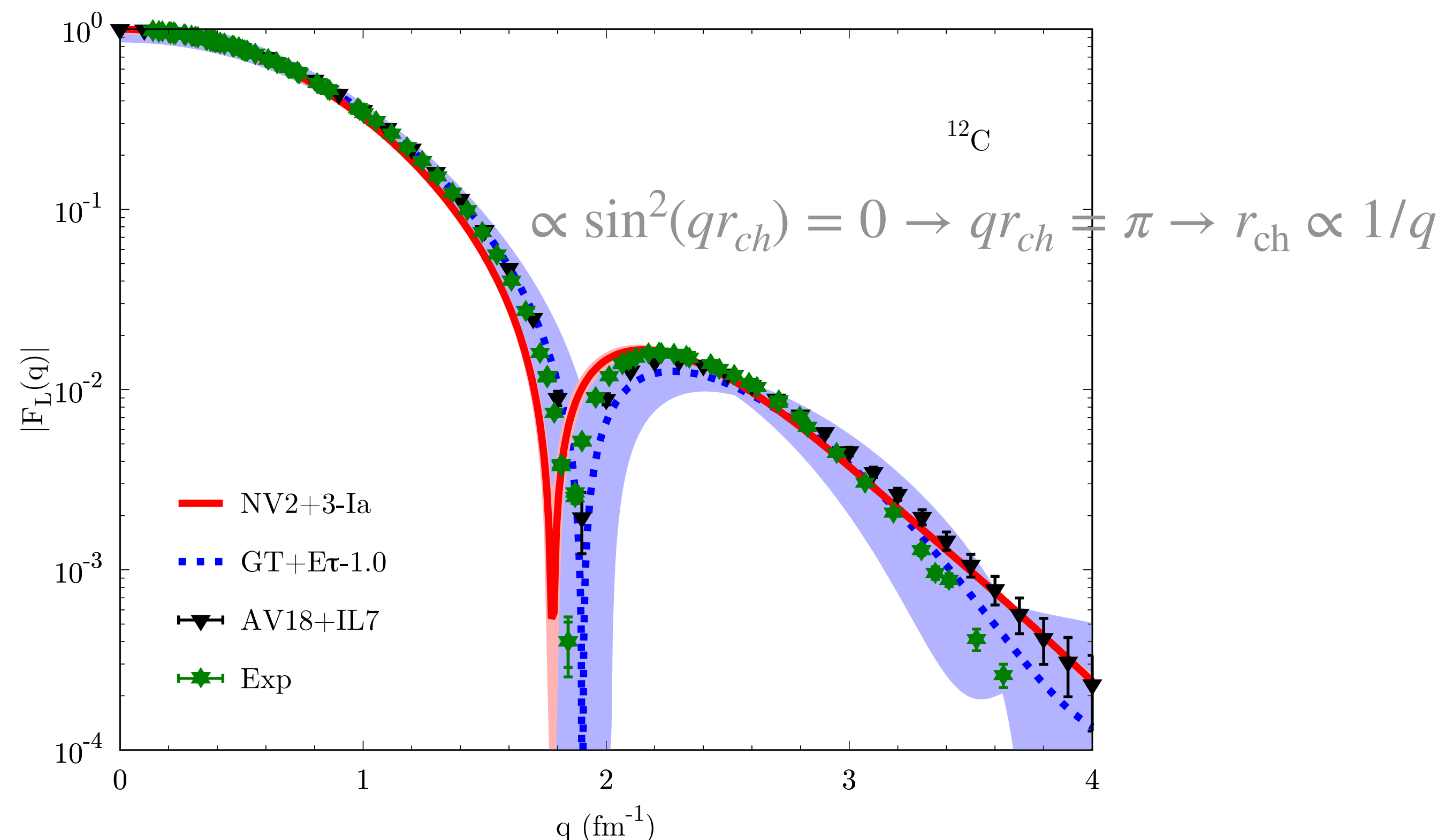
- For symmetric nuclei  $N = Z$  nuclei, proton and neutron densities are the same.
- $s$ -shell nuclei ( $A \leq 4$ ) exhibit large peaks at small separation, while the  $p$ -shell nuclei ( $A \geq 6$ ) are much reduced at small  $r$  and more spread out: due to cluster structure of these light  $p$ -shell nuclei puts the center of mass of these nuclei in between clusters and thus reduces the central density.
- Densities are not observables but single-nucleon density can be related to longitudinal (charge) form factor physical quantity experimentally accessible via electron-nucleon scattering processes

# Charge form factors in A=6 and A=12

Longitudinal form factor for  ${}^6\text{Li}$



Longitudinal form factor for  ${}^{12}\text{C}$



The charge form factor can be expressed as the **ground-state expectation value of the one-body charge operator**, which, ignoring small spin-orbit contributions in the one-body current, results in the following expression:

$$F_L(q) = \frac{1}{Z} \frac{G_E^p(Q_{el}^2) \tilde{\rho}_p(q) + G_E^n(Q_{el}^2) \tilde{\rho}_n(q)}{\sqrt{1 + Q_{el}^2/(4m_N^2)}}$$

$\tilde{\rho}_N(q)$ : the Fourier transform of  $\rho_N(r)$

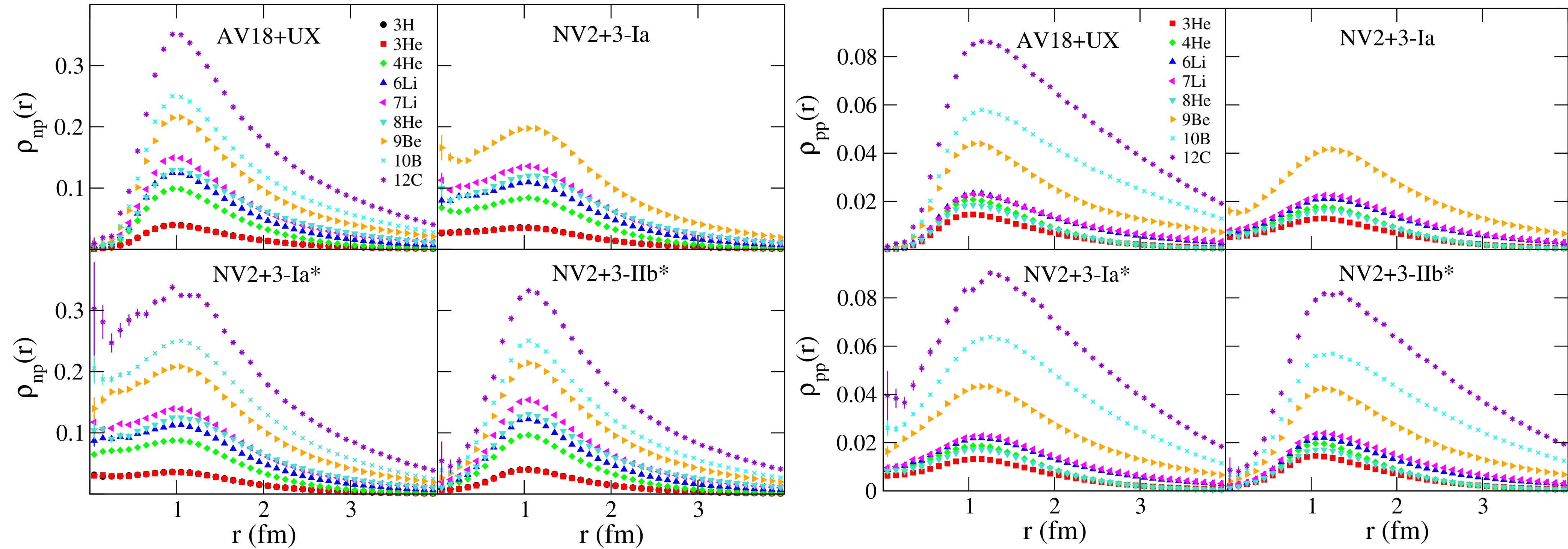
$$Q_{el}^2 = \mathbf{q}^2 - \omega_{el}^2 \quad \omega_{el} = \sqrt{q^2 + m_A^2} - m_A$$

$G_E^N(Q^2)$ : electric nucleonic form factor



# Nuclear structure: two-nucleon densities

- In QMC methods, two-nucleon densities are calculated as: 
$$\rho_{NN}(r) = \frac{1}{4\pi r^2} \langle \Psi | \sum_{i < j} \mathcal{P}_{N_i} \mathcal{P}_{N_j} \delta(r - |\mathbf{r}_i - \mathbf{r}_j|) | \Psi \rangle$$



- Within a fixed interaction model,  $\rho_{NN}(r)$  at  $r \lesssim 1.5$  fm for various nuclei exhibit a similar behavior: cooperation of the short-range repulsion and the intermediate-range tensor attraction of the NN interaction, with the tensor force being responsible of the large overshooting at  $r \sim 1.0$  fm between a  $np$  pair compared to a  $pp$  pair.
- While the short-distance behavior is the same for all nuclei, it differs for each interaction. Indeed, the probability of finding two nucleons at short distances is finite for the "soft" NV2+3-Ia and NV2+3-Ia\* chiral models, but approaches to zero as we progress from the "hard" local chiral interaction NV2+3-IIb\* to the "hardest" phenomenological AV18+UX.

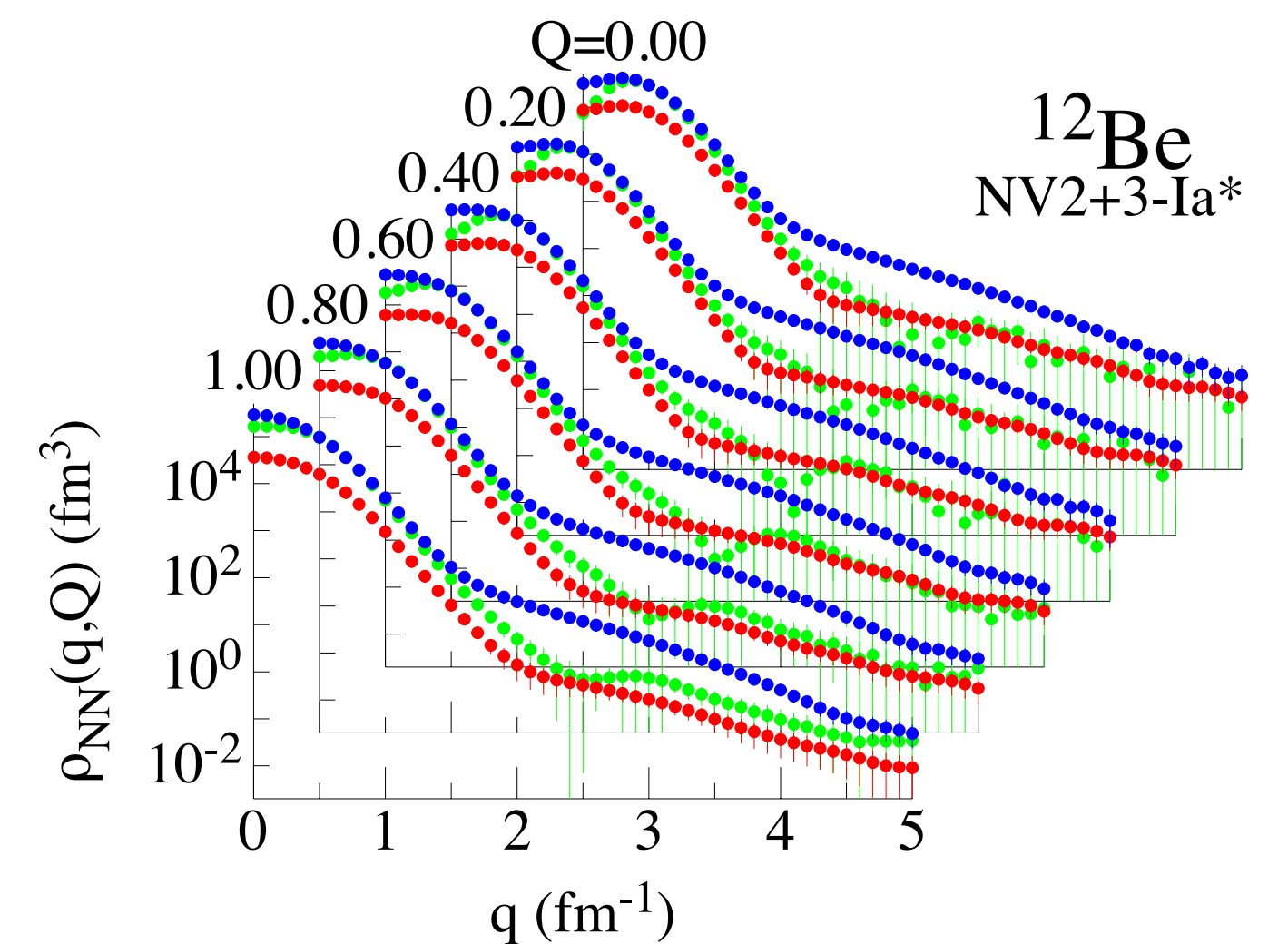
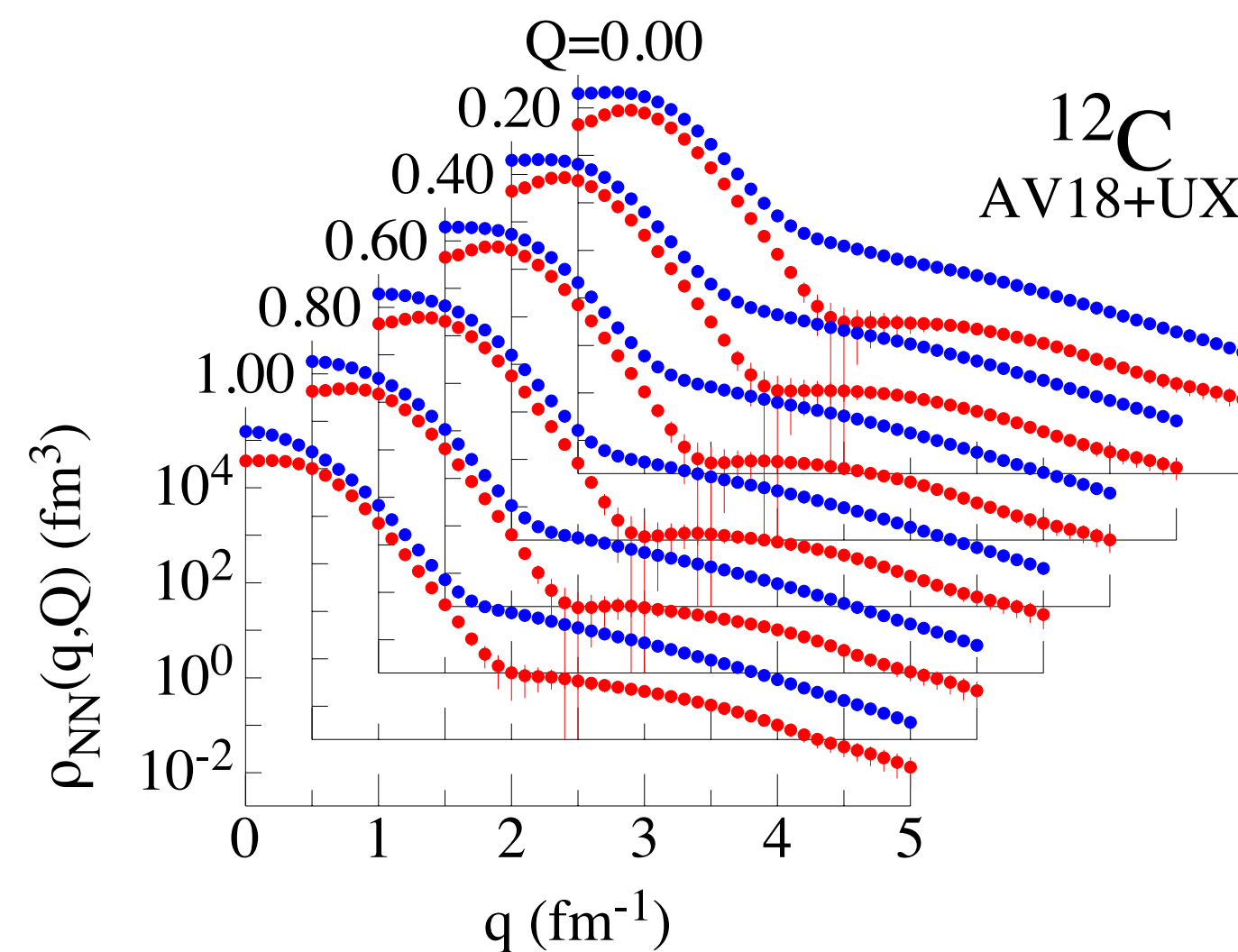
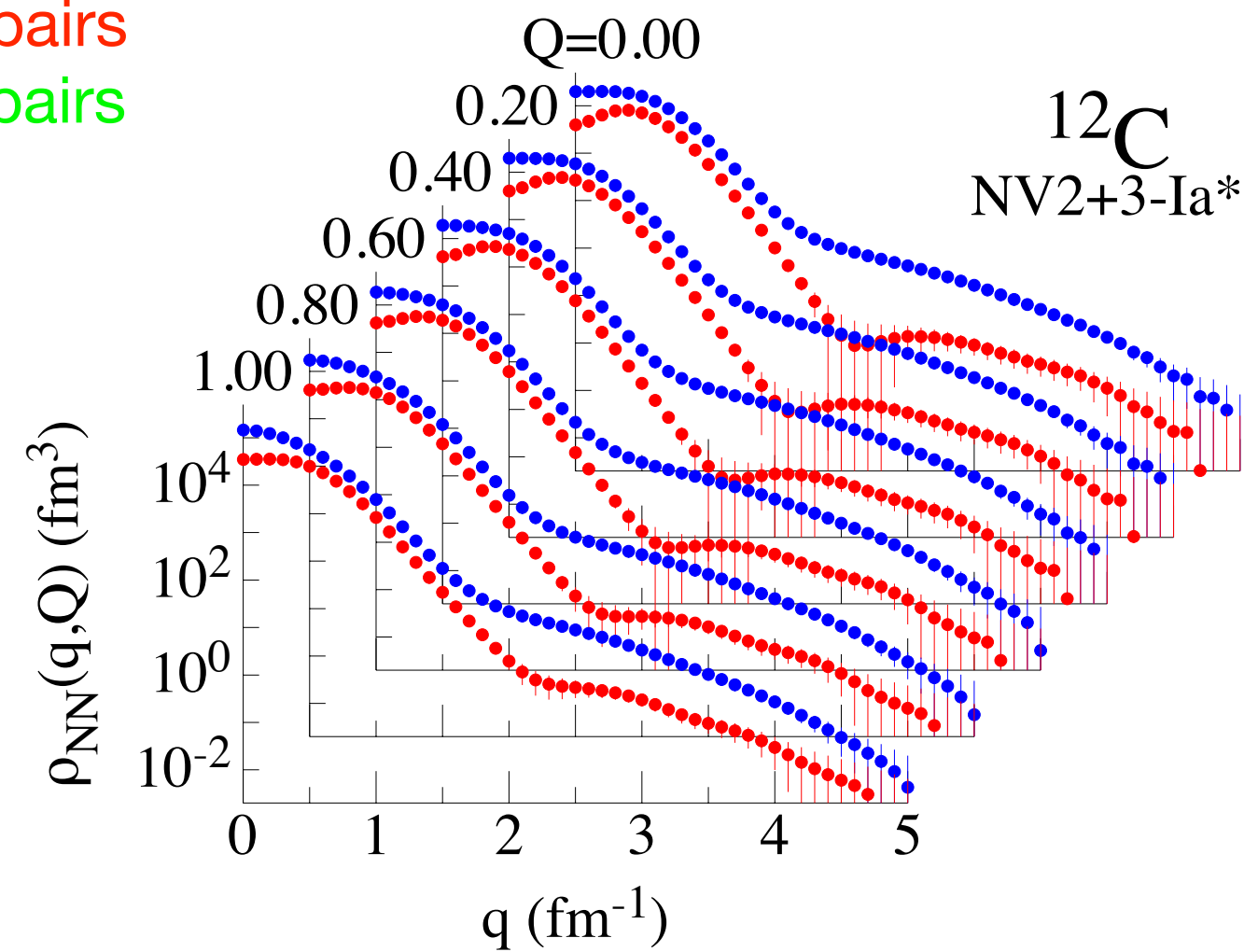
# Nuclear structure: two-nucleon densities

- The probability of finding two nucleons in a nucleus with relative momentum  $\mathbf{q}$  and total-center-of-mass momentum  $\mathbf{Q}$  in a spin-isospin projection

$$\rho_{ST}(\mathbf{q}, \mathbf{Q}) = \int d\mathbf{r}'_1 d\mathbf{r}_1 d\mathbf{r}'_2 d\mathbf{r}_2 d\mathbf{r}_3 \cdots d\mathbf{r}_A \psi_{JM_J}^\dagger(\mathbf{r}'_1, \mathbf{r}'_2, \mathbf{r}_3, \dots, \mathbf{r}_A) e^{-i\mathbf{q}\cdot(\mathbf{r}_{12}-\mathbf{r}'_{12})} \\ \times e^{-i\mathbf{Q}\cdot(\mathbf{R}_{12}-\mathbf{R}'_{12})} P_{ST}(12) \psi_{JM_J}(\mathbf{r}_1, \mathbf{r}_2, \mathbf{r}_3, \dots, \mathbf{r}_A)$$

The total normalization is:  $N_{ST} = \int \frac{d\mathbf{q}}{(2\pi)^3} \frac{d\mathbf{Q}}{(2\pi)^3} \rho_{ST}(\mathbf{q}, \mathbf{Q})$

np pairs  
pp pairs  
nn pairs

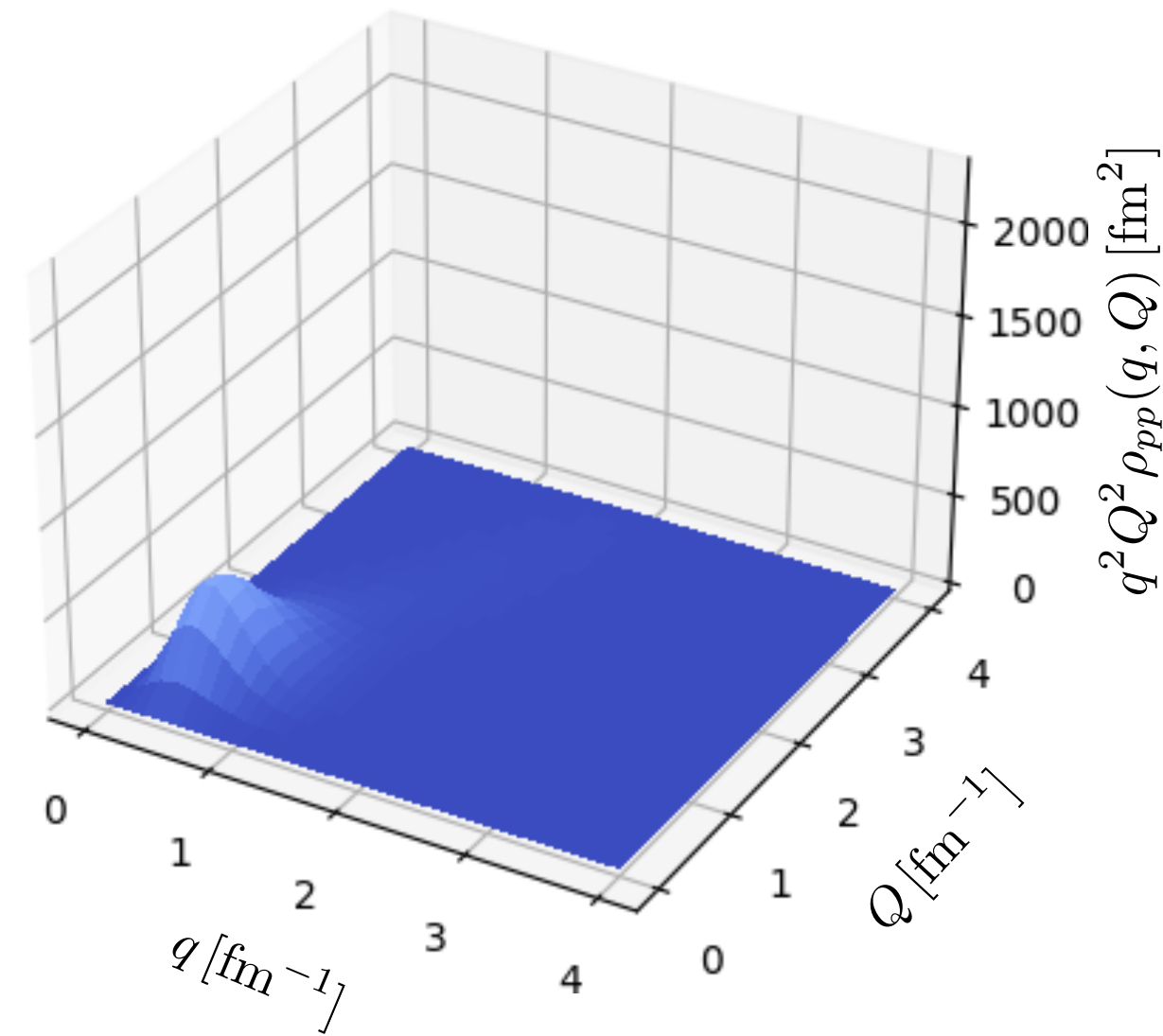
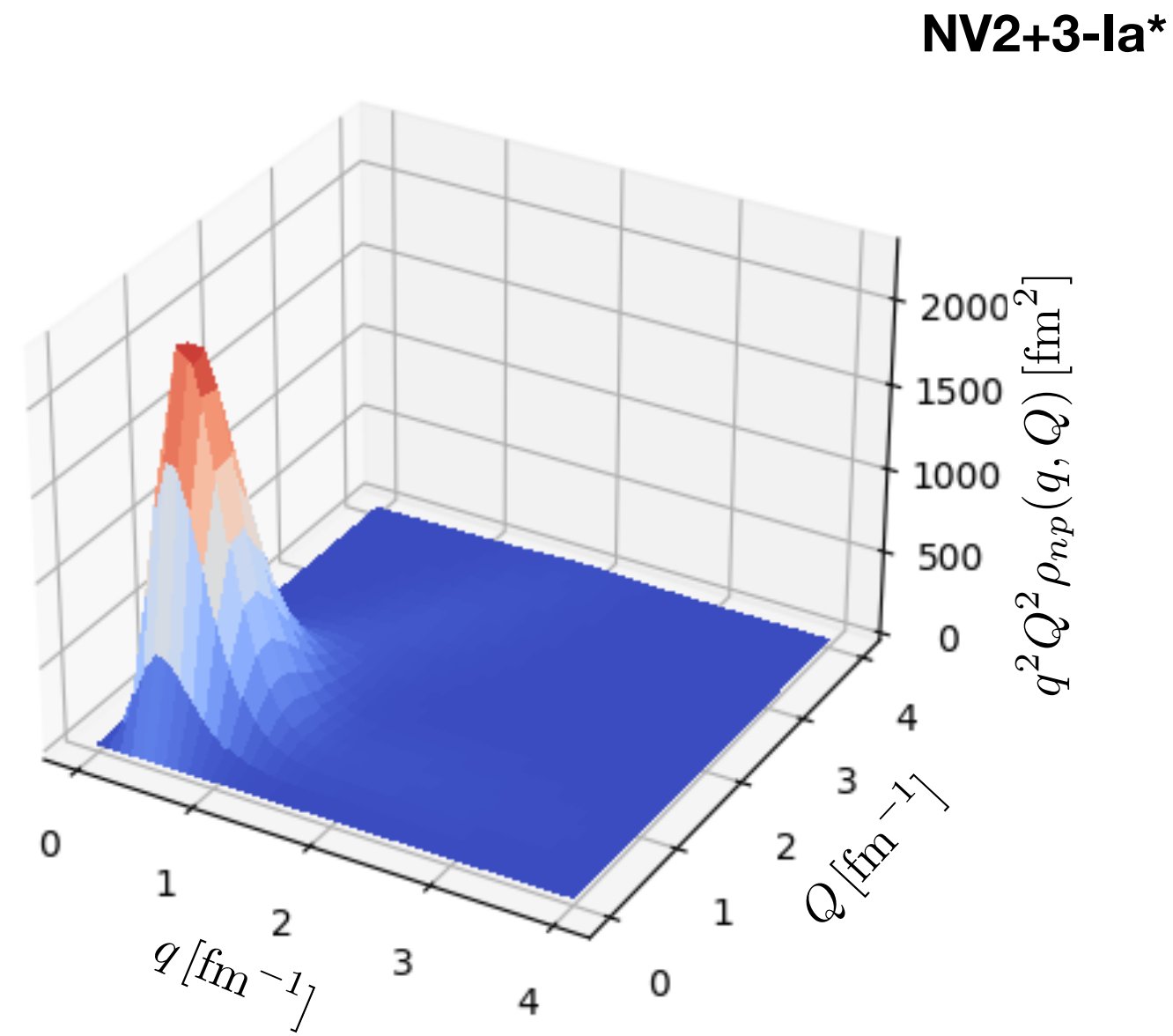
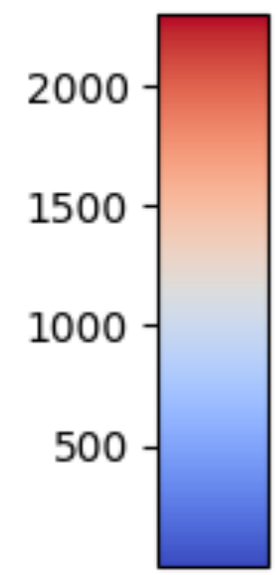


- In  $^{12}\text{C}$  both Hamiltonian exhibit the large pn/pp ratio around  $q = 2 \text{ fm}^{-1}$  for small  $Q$ , which gradually reduces as  $Q$  increases. They also show the high-momentum tail in  $q$ , but it decays more rapidly with increasing  $q$  for the “soft” chiral force.



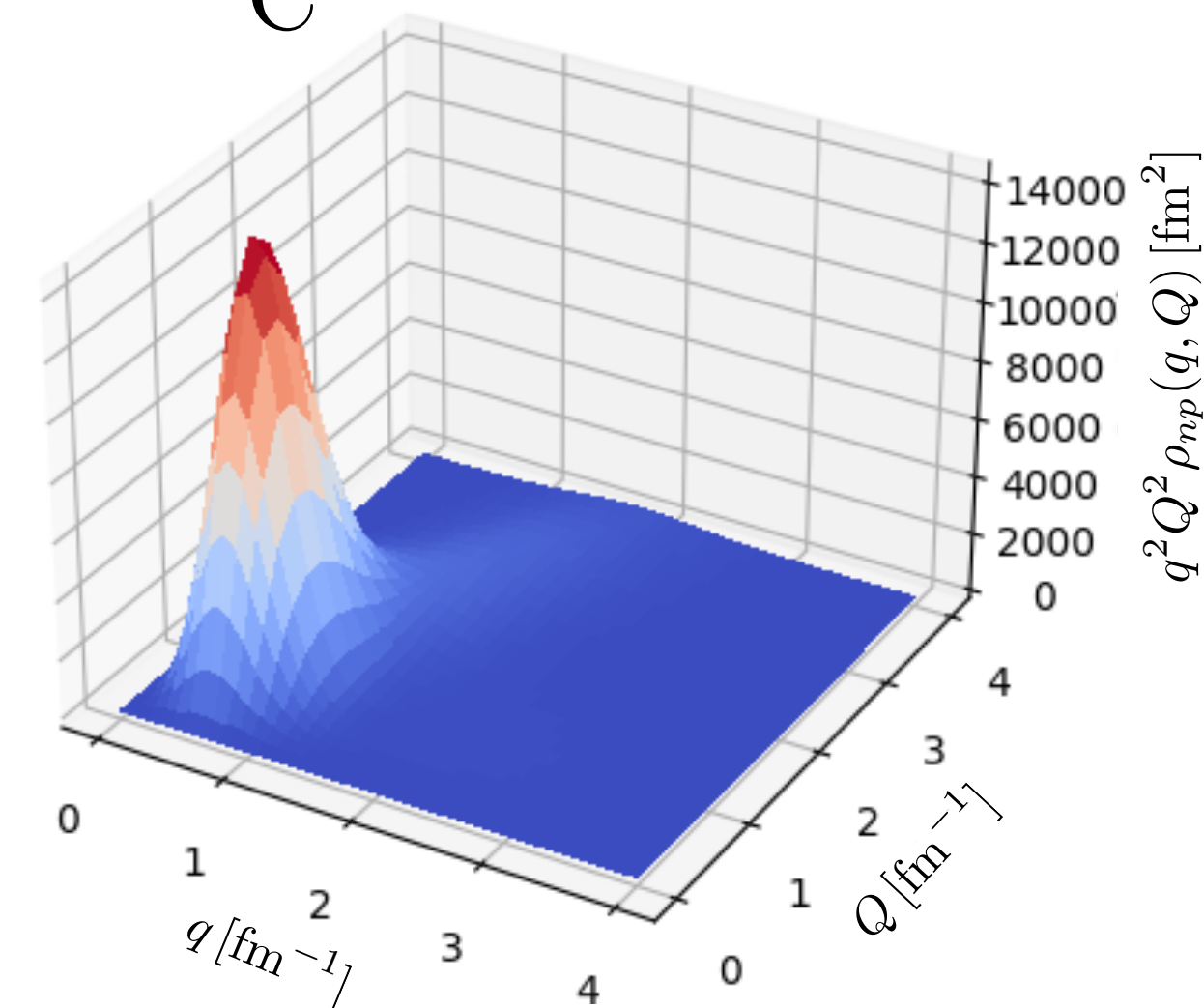
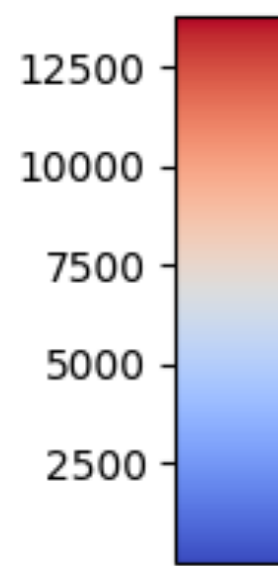
# Nuclear structure: two-nucleon momentum distribution

${}^4\text{He}$

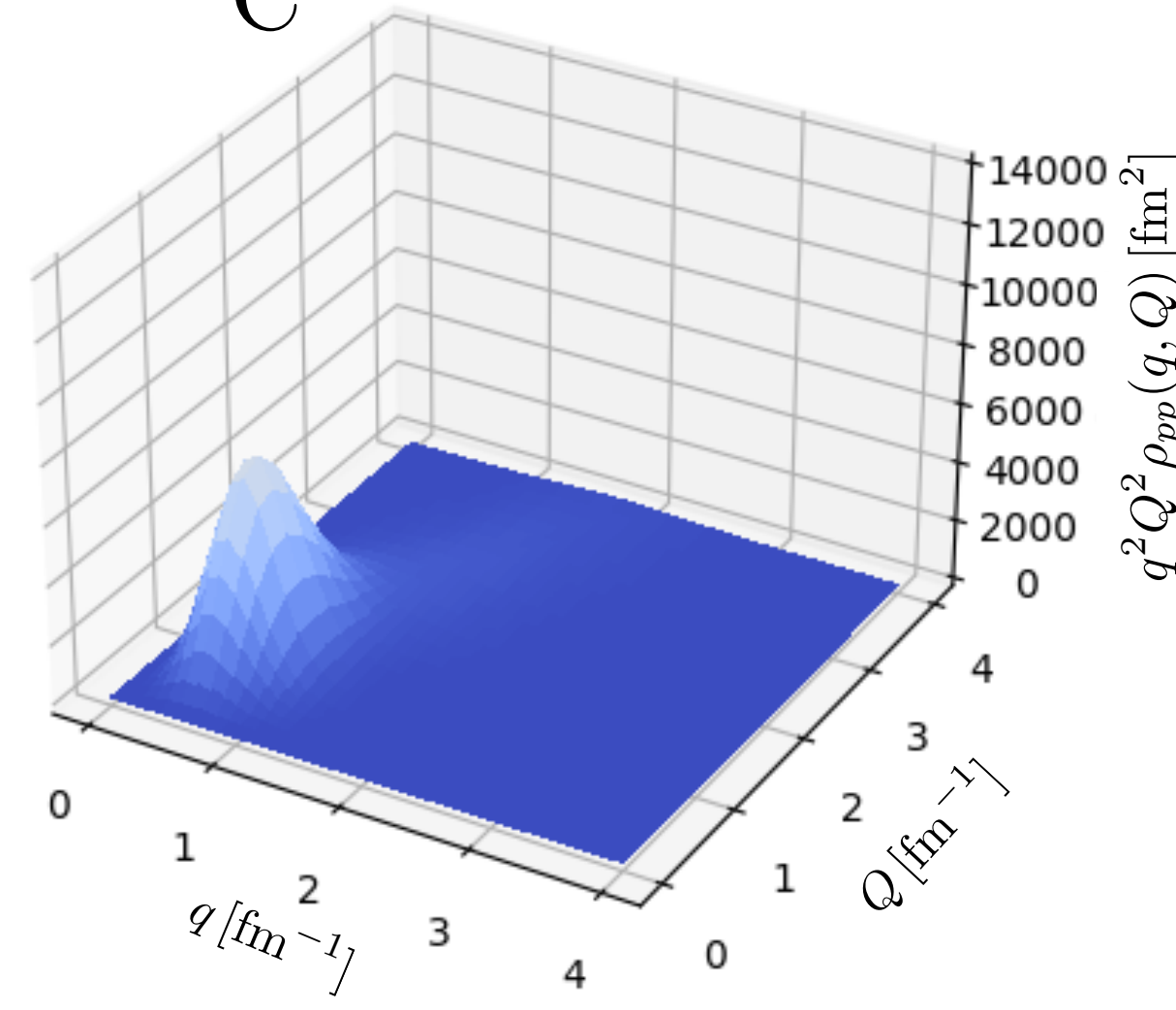


**AV18UX**

${}^{12}\text{C}$



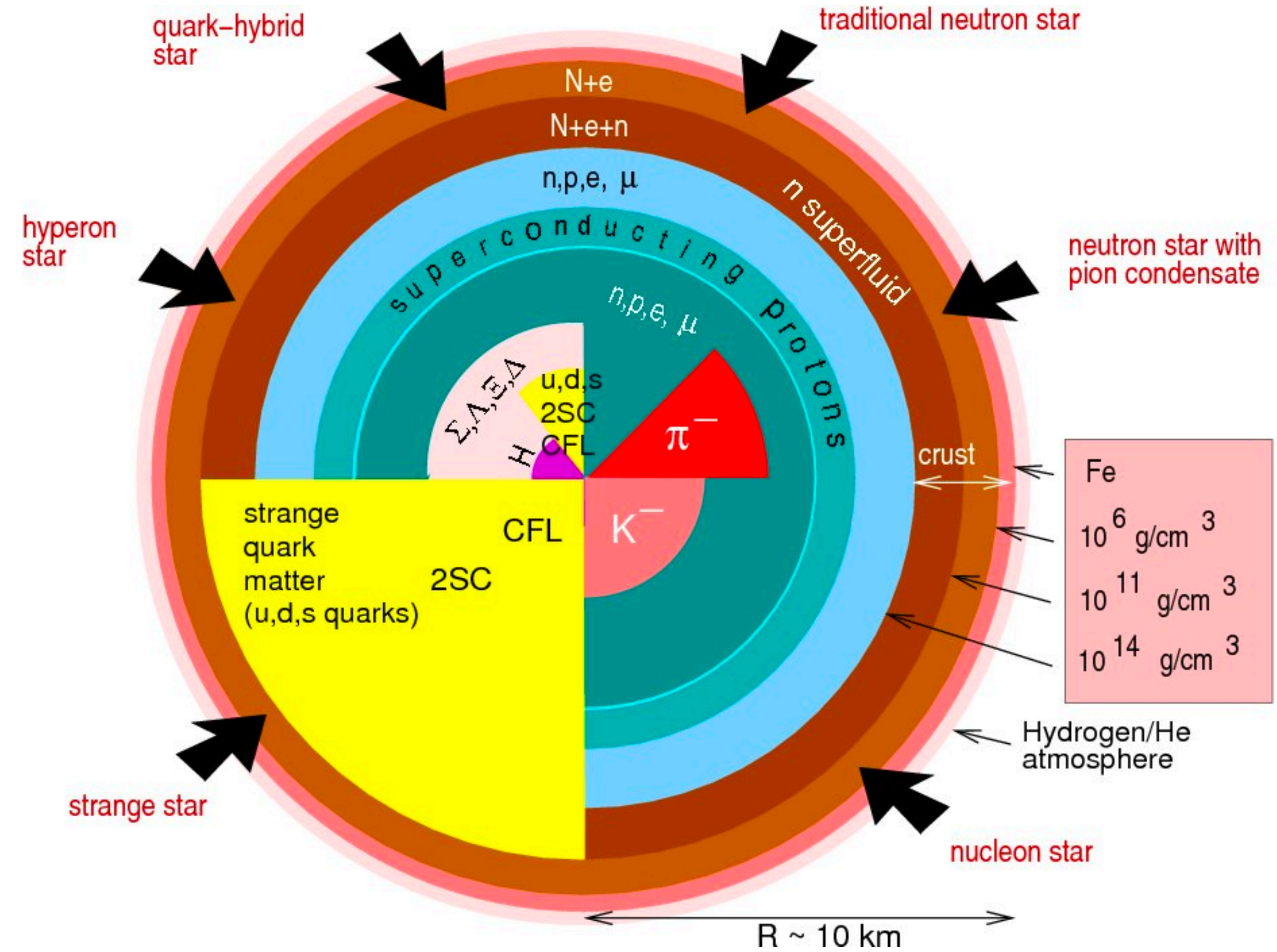
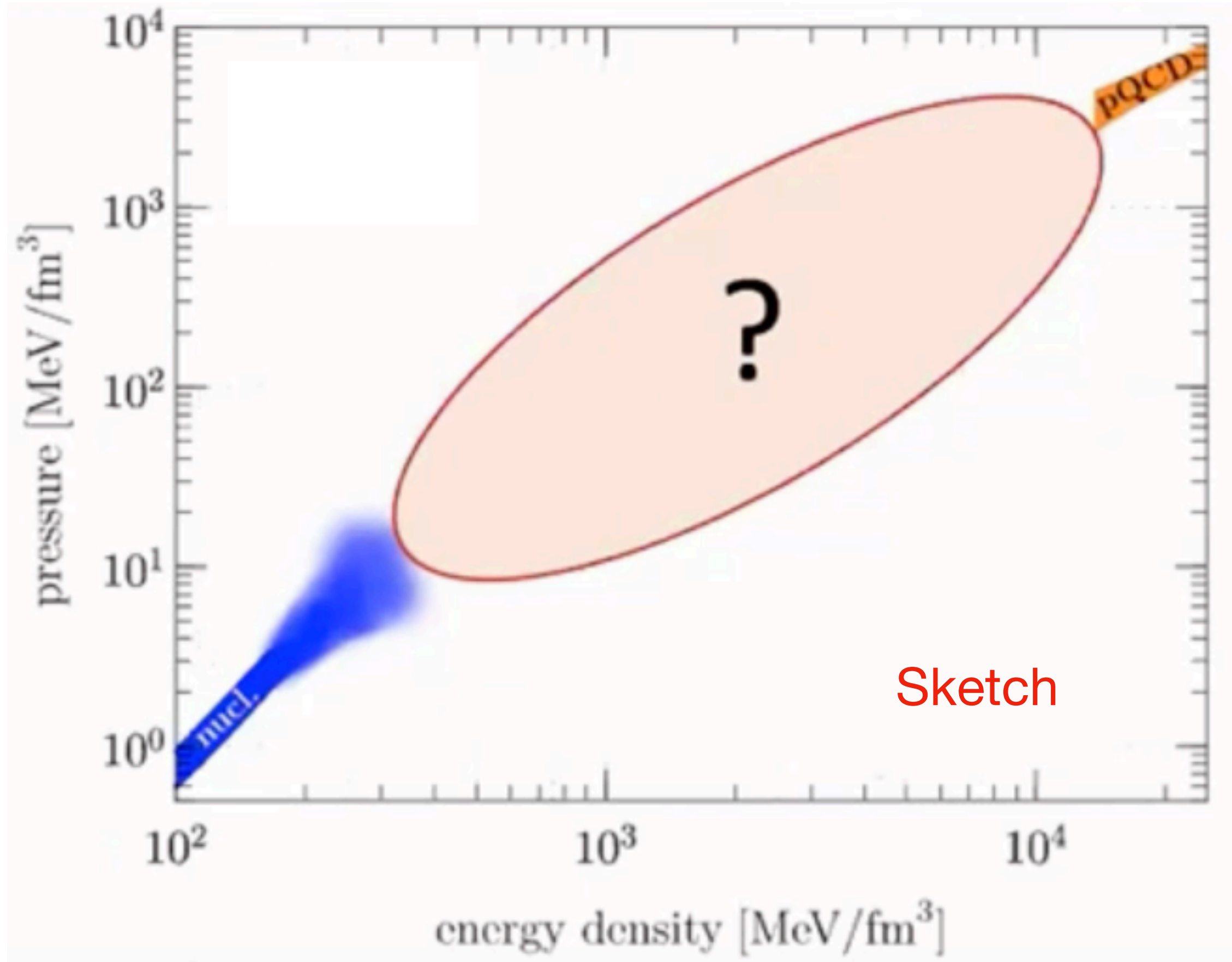
${}^{12}\text{C}$



- Tables and figures that tabulate the single-nucleon momentum distribution (including proton and neutron spin momentum distribution) and two-nucleon momentum distribution (including pair distributions in different combinations of ST) will be available online
- A new capability in the VMC code: constraint in the momentum distribution according to pair separation distance



# Dense matter equation of state of neutron matter



Constraints:

At low density from nuclear theory and experiment

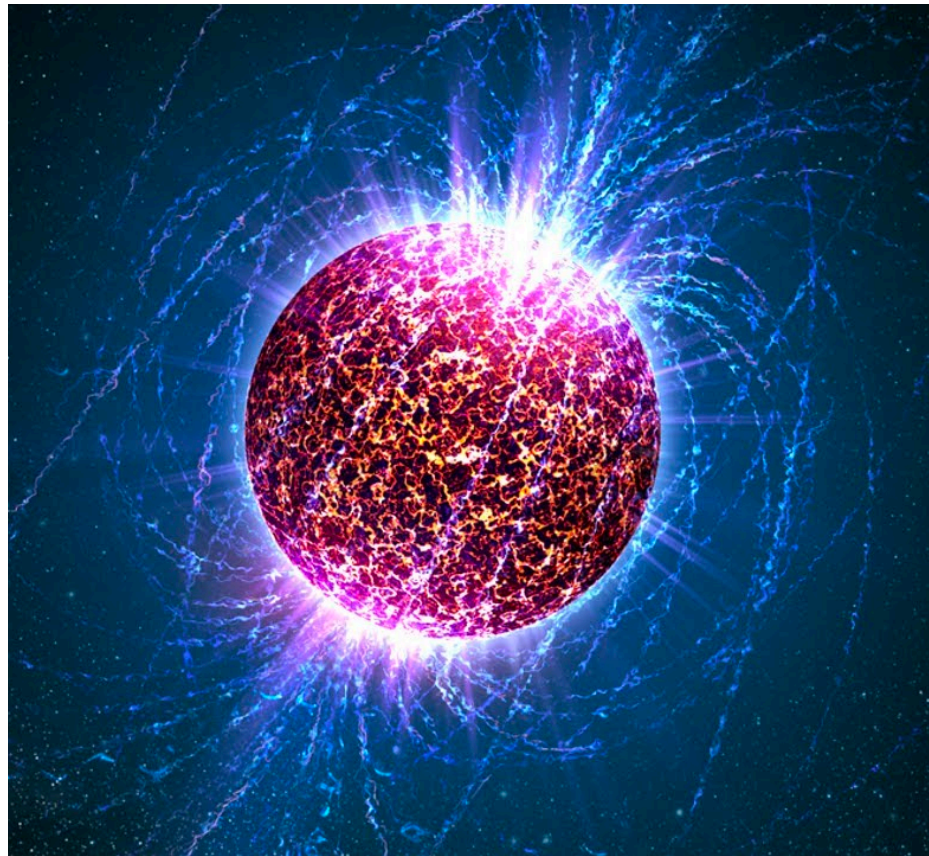
At very high density from pQCD

No robust constraint at intermediate densities from nuclear physics

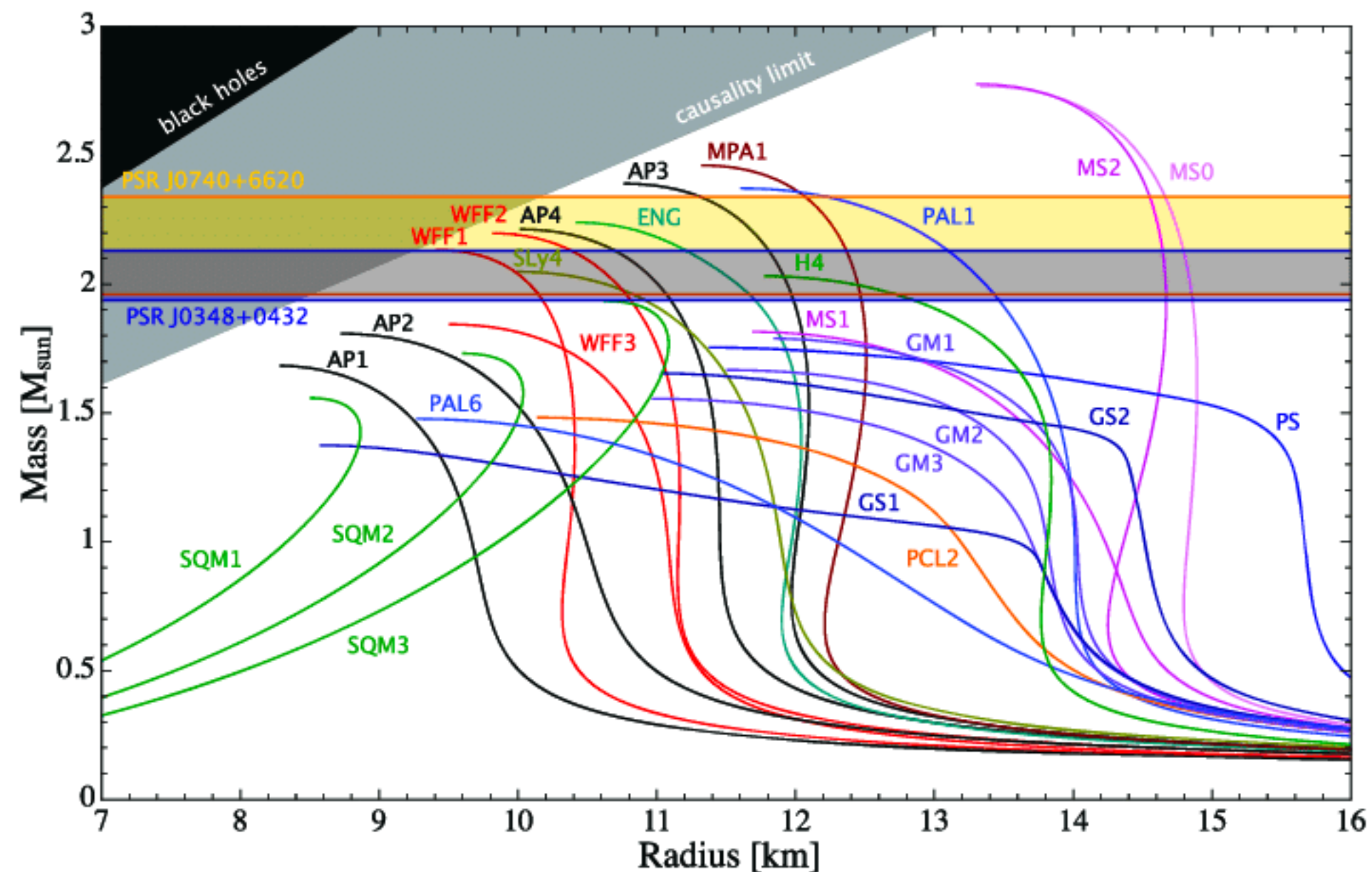
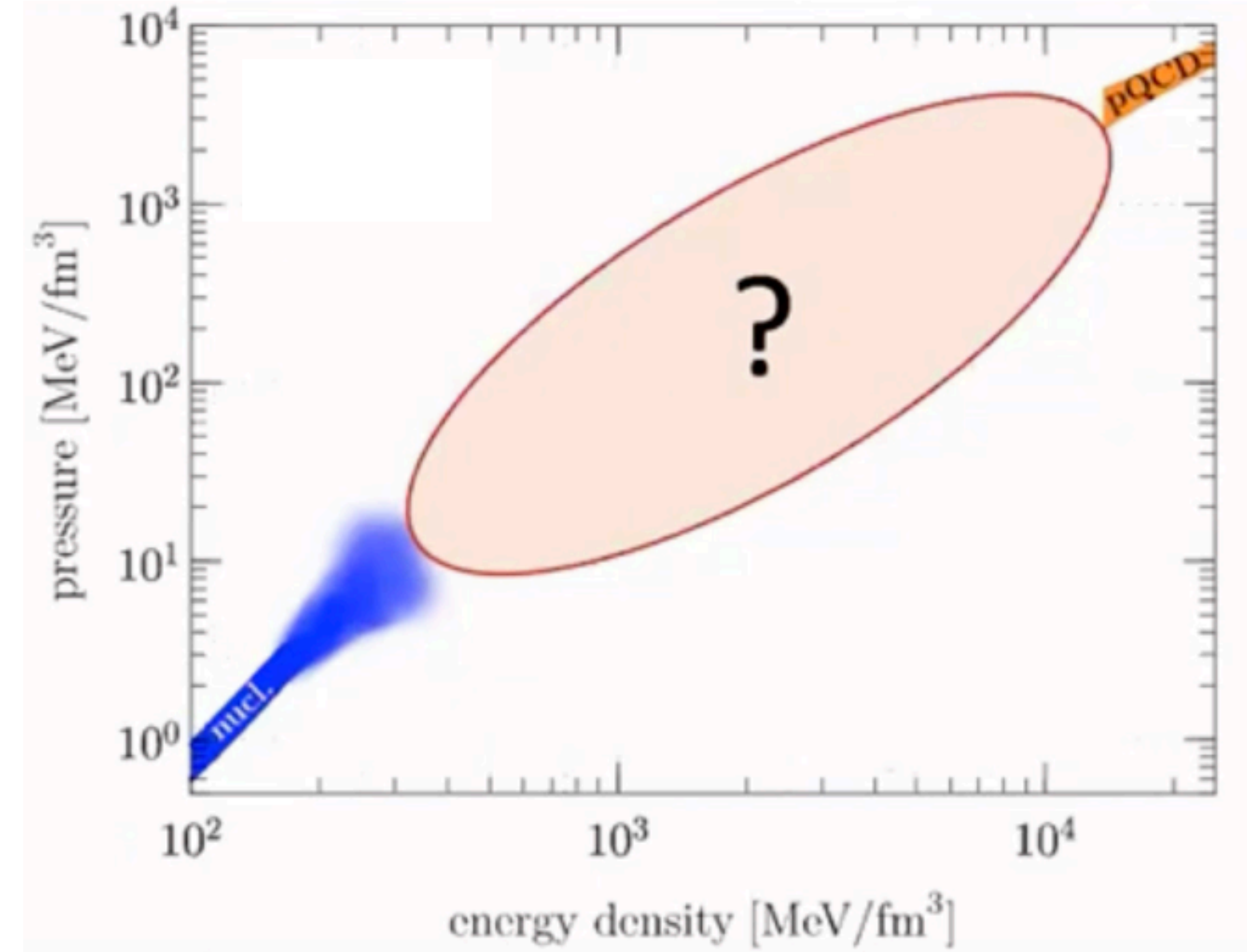


# Dense matter equation of state of neutron matter

- The EoS of pure neutron matter (PNM): neutrons stars



- ▶ Compact objects:  $R \sim 10\text{km}$ ,
- ▶ Composed predominantly of neutrons between the inner crust and the outer core
- ▶ NS from gravitational collapse of a massive star after a supernova explosion



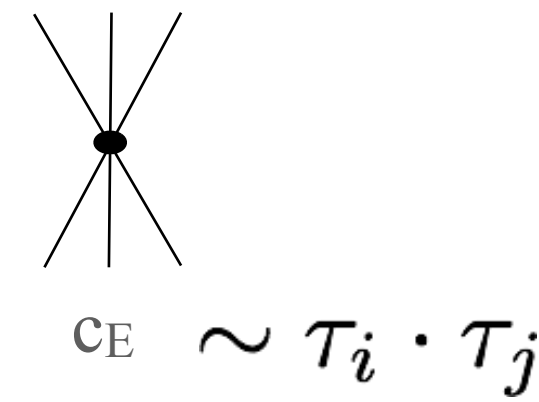
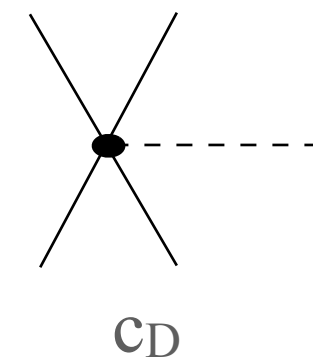
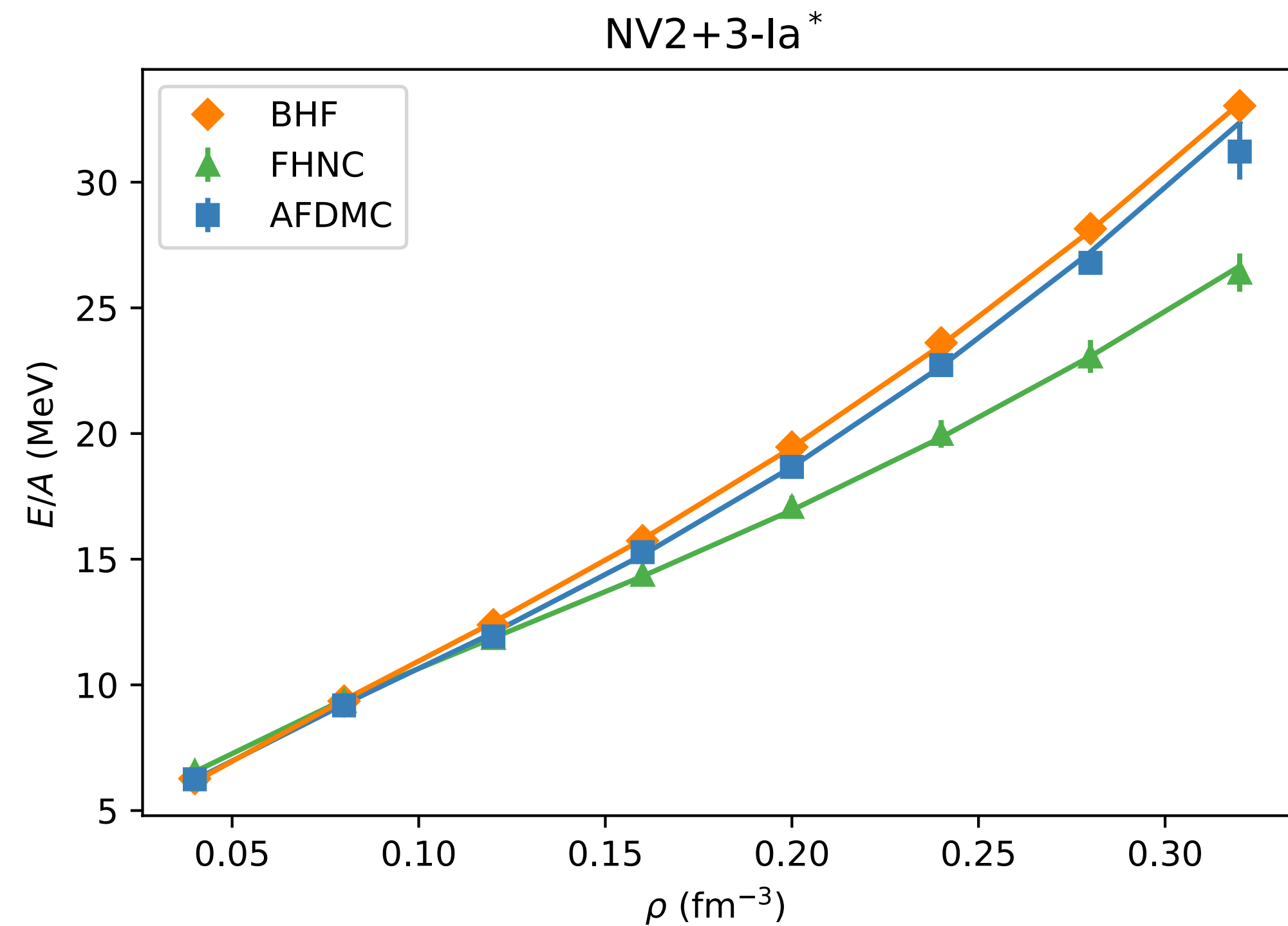
Constraints:

- At low density from nuclear theory and experiment
- At very high density from pQCD
- No robust constraint at intermediate densities from nuclear physics



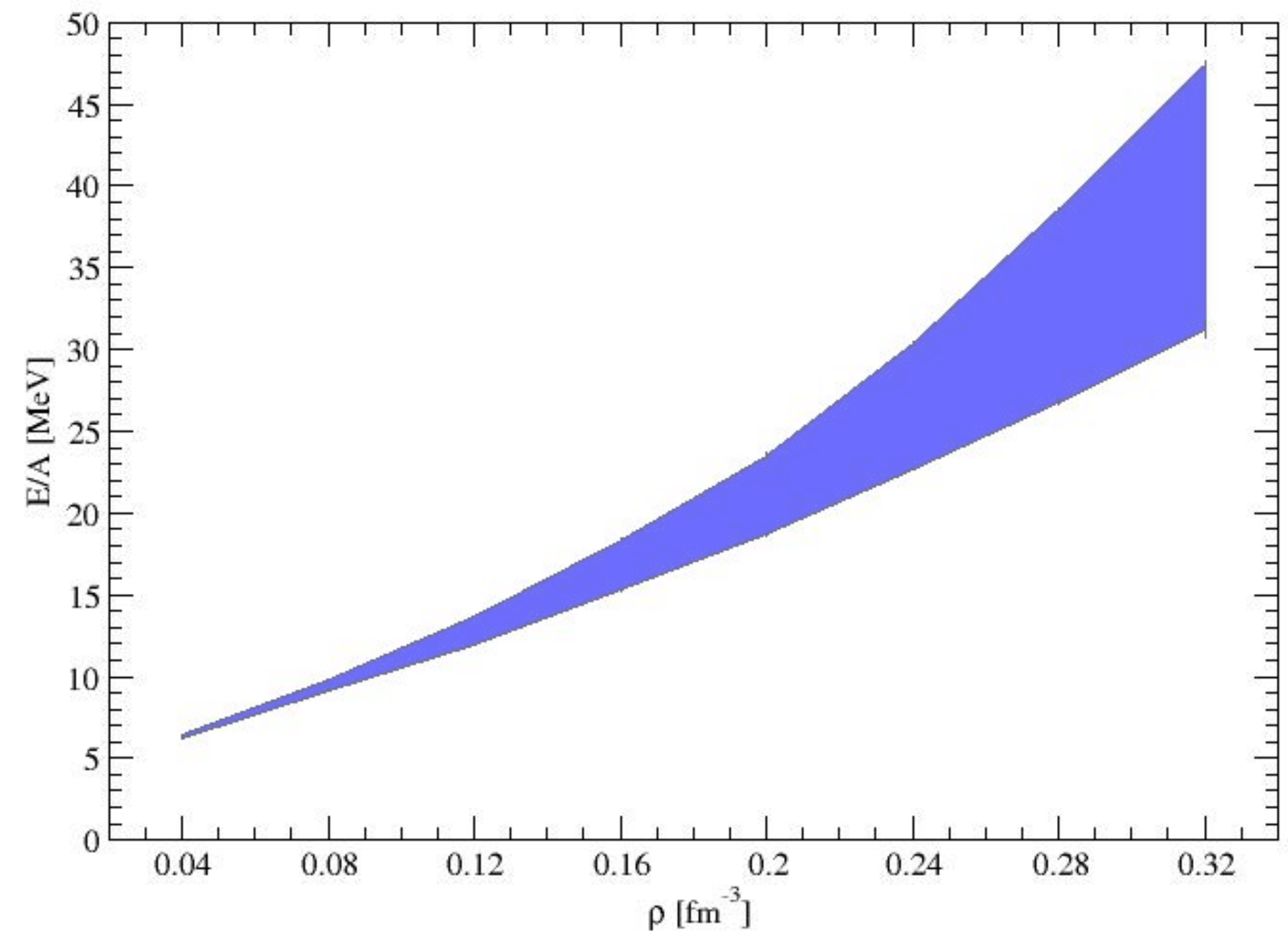
# Neutron matter with realistic NN+3N potentials

- Benchmark calculations between BHF, FHNC/SOC, AFDMC-UP for both the AV18 and chiral-EFT interactions



NV2+3s\*

Model	$c_D$	$c_E$
Ia*	-0.635(255)	-0.09(8)
Ib*	-4.705(285)	0.550(150)
IIa*	-0.610(280)	-0.350(100)
IIb*	-5.250(310)	0.05(180)

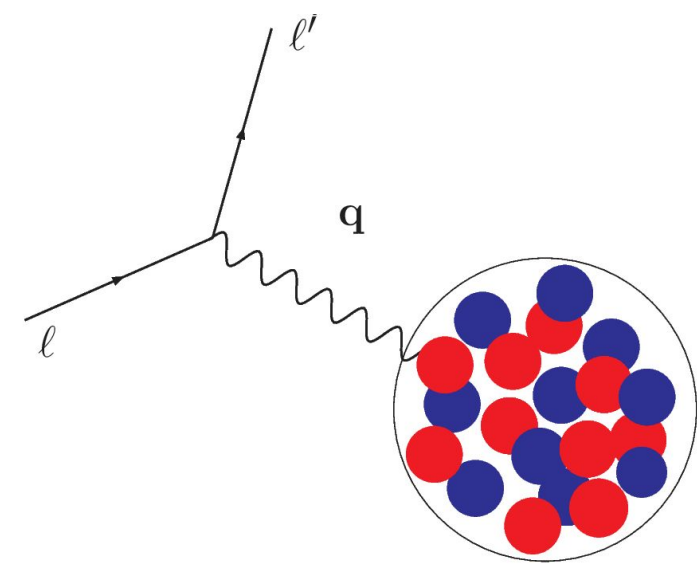


- AFDMC-UC, BHF, FHNC/SOC are very close to each other up to  $\rho = \rho_0$  ( $\sim 1$  MeV)
- FHNC/SOC is below AFDMC and BHF at higher density; due to limited three-body terms into the cluster expansion  $\rho = 2\rho_0$  ( $\sim 6$  MeV)
- Model dependence of the EOS at three-body level  $\rho = 2\rho_0$  ( $\sim 16$  MeV)
- The exp error on the 3H beta decays in the NV2+3s\* (numbers in parenthesis) is not propagated yet

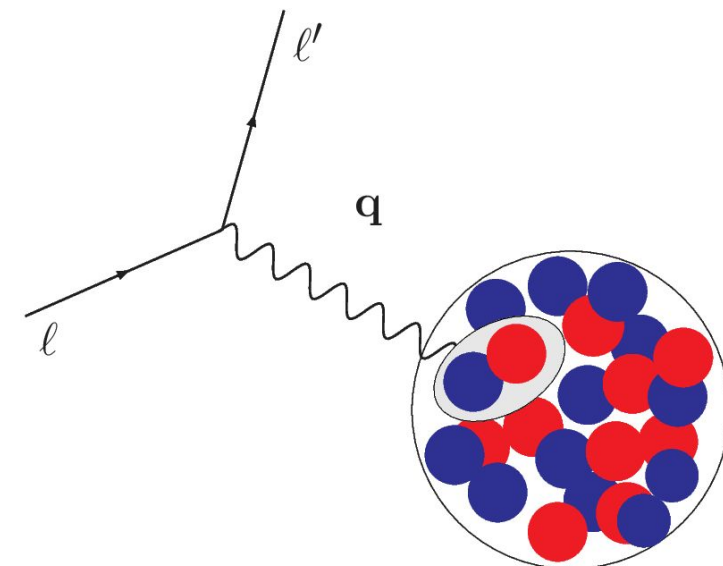
MP *et al.* Phys. Rev. C 101, 045801 (2020)  
 Lovato, MP *et al.* arxiv 2202.10293 (2022)

# Many-body Nuclear Electroweak Currents

- Electroweak structure and reactions:



one-body



two-body

- Accurate understanding of the electroweak interactions of external probes with **nucleons**, **correlated nucleon-pairs**,...
- Two-body currents are a manifestation of two-body correlations
- Electromagnetic two-body currents are required to satisfy current conservation

$$\mathbf{q} \cdot \mathbf{j} = [H, \rho] = [t_i + v_{ij} + V_{ijk}, \rho]$$

- Meson exchange currents: [R. Schiavilla et al., PRC 45, 2628 \(1992\)](#), [Marcucci et al. PRC 72, 014001 \(2005\)](#), [L. Marcucci et al., PRC 78, 065501 \(2008\)](#)
- Chiral EFT currents: [Park et al. NPA 596, 515 \(1996\)](#); [Pastore et al. PRC 78, 064002 \(2008\)](#), [PRC 80, 034004 \(2009\)](#); [Piarulli et al. PRC 87, 014006 \(2013\)](#), [Baroni et al. PRC 93, 015501 \(2016\)](#); [Phillips et al. PRC 72, 014006 \(2005\)](#), [Kölling et al. PRC 80, 045502 \(2009\)](#), [PRC 84, 054008](#), [PRC 86, 047001 \(2012\)](#); [Krebs et al., Ann. Phys. 378, 317 \(2017\)](#)

- Electroweak form factors
- Magnetic moments and radii
- Electroweak Response functions
- Radiative/weak captures
- G.T. matrix elements involved in beta decays
- .....

Nuclear charge operator

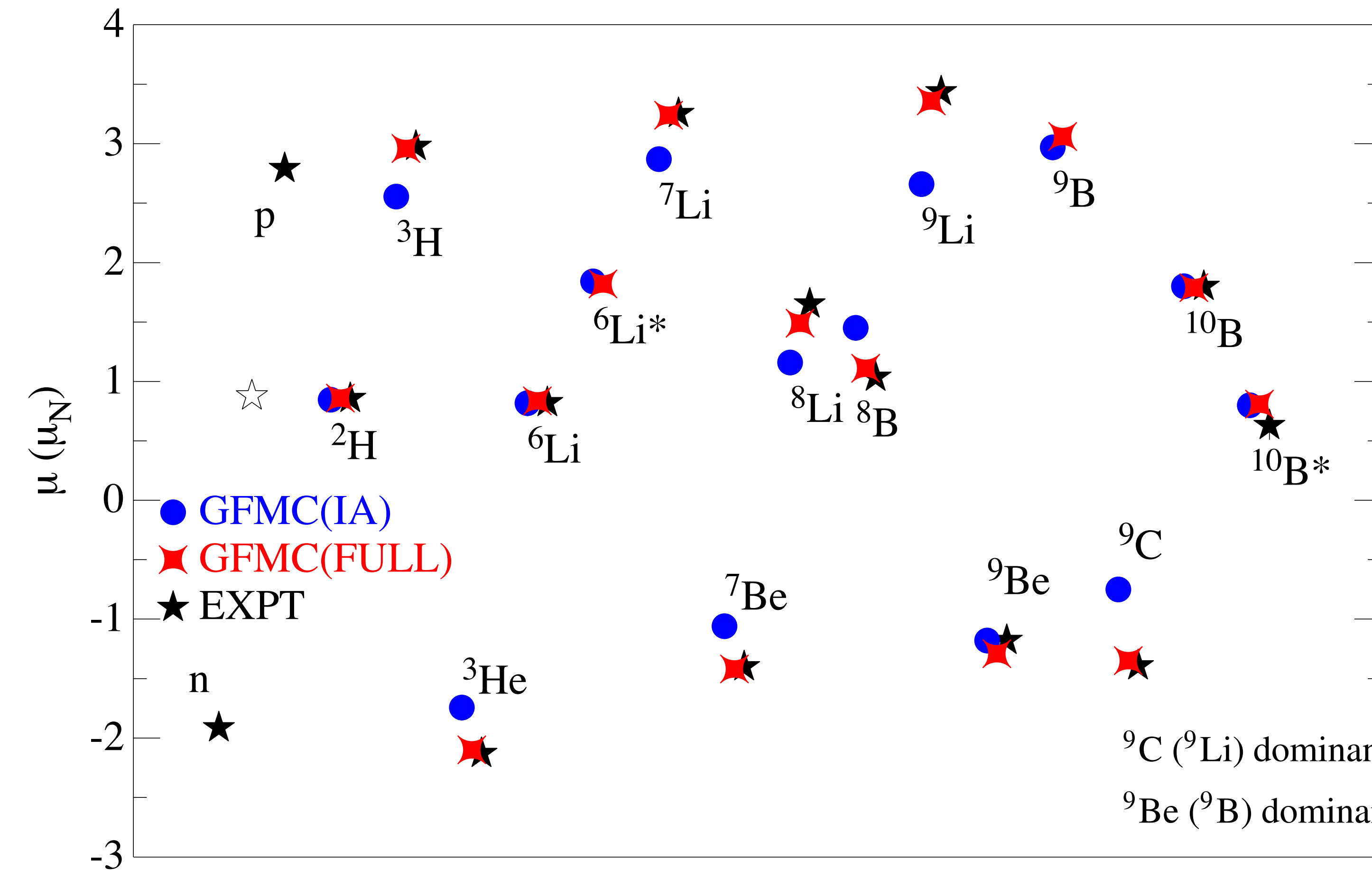
$$\rho = \sum_{i=1}^A \rho_i + \sum_{i<j} \rho_{ij} + \dots$$

Nuclear vector operator

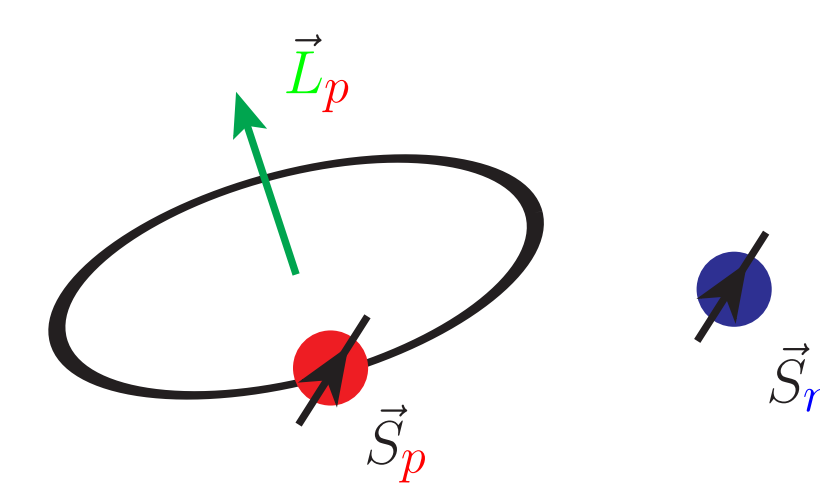
$$\mathbf{j} = \sum_{i=1}^A \mathbf{j}_i + \sum_{i<j} \mathbf{j}_{ij} + \dots$$

# Magnetic moment and EM decay

- GFMC calculations using AV18/IL7 (rather than chiral) and EM  $\chi$ EFT currents— hybrid calculation



$$\mu(\text{IA}) = \mu_N \sum_i [(L_i + g_p S_i)(1 + \tau_{i,z})/2 + g_n S_i(1 - \tau_{i,z})/2]$$



$$\langle J_f^\pi, M_f | \mu^{\text{MEC}} | J_i^\pi, M_i \rangle = -i \lim_{q \rightarrow 0} \frac{2 m_N}{q} \langle J_f^\pi, M_f | j_y^{\text{MEC}}(q \hat{\mathbf{x}}) | J_i^\pi, M_i \rangle$$

${}^9\text{C}$  ( ${}^9\text{Li}$ ) dominant spatial symmetry [s.s.] = [432] = [ $\alpha$ ,  ${}^3\text{He}({}^3\text{H}), pp(nn)$ ]  $\rightarrow$  Large MEC

${}^9\text{Be}$  ( ${}^9\text{B}$ ) dominant spatial symmetry [s.s.] = [441] = [ $\alpha$ ,  $\alpha, n(p)$ ]

Pastore *et al.* PRC 87, 035503 (2013)

*Electromagnetic data are explained when two-body correlations and currents are accounted for!*

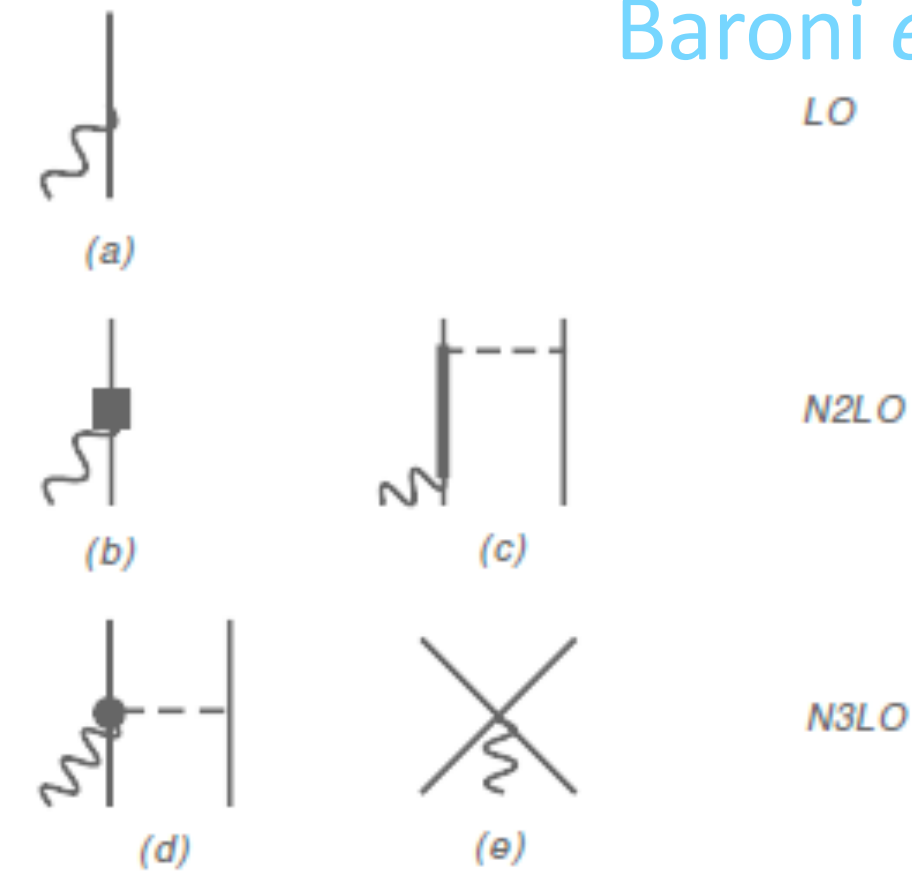
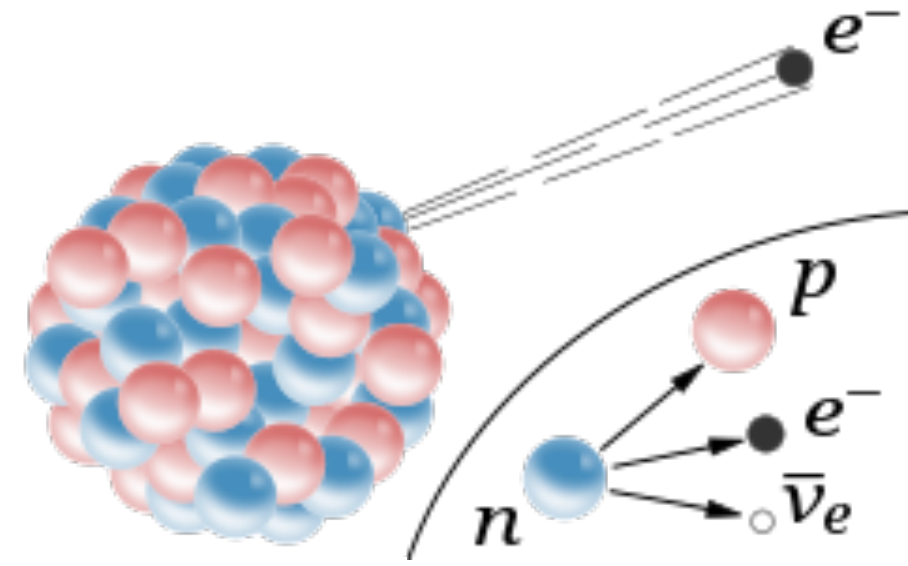


# Single-Beta decay matrix elements

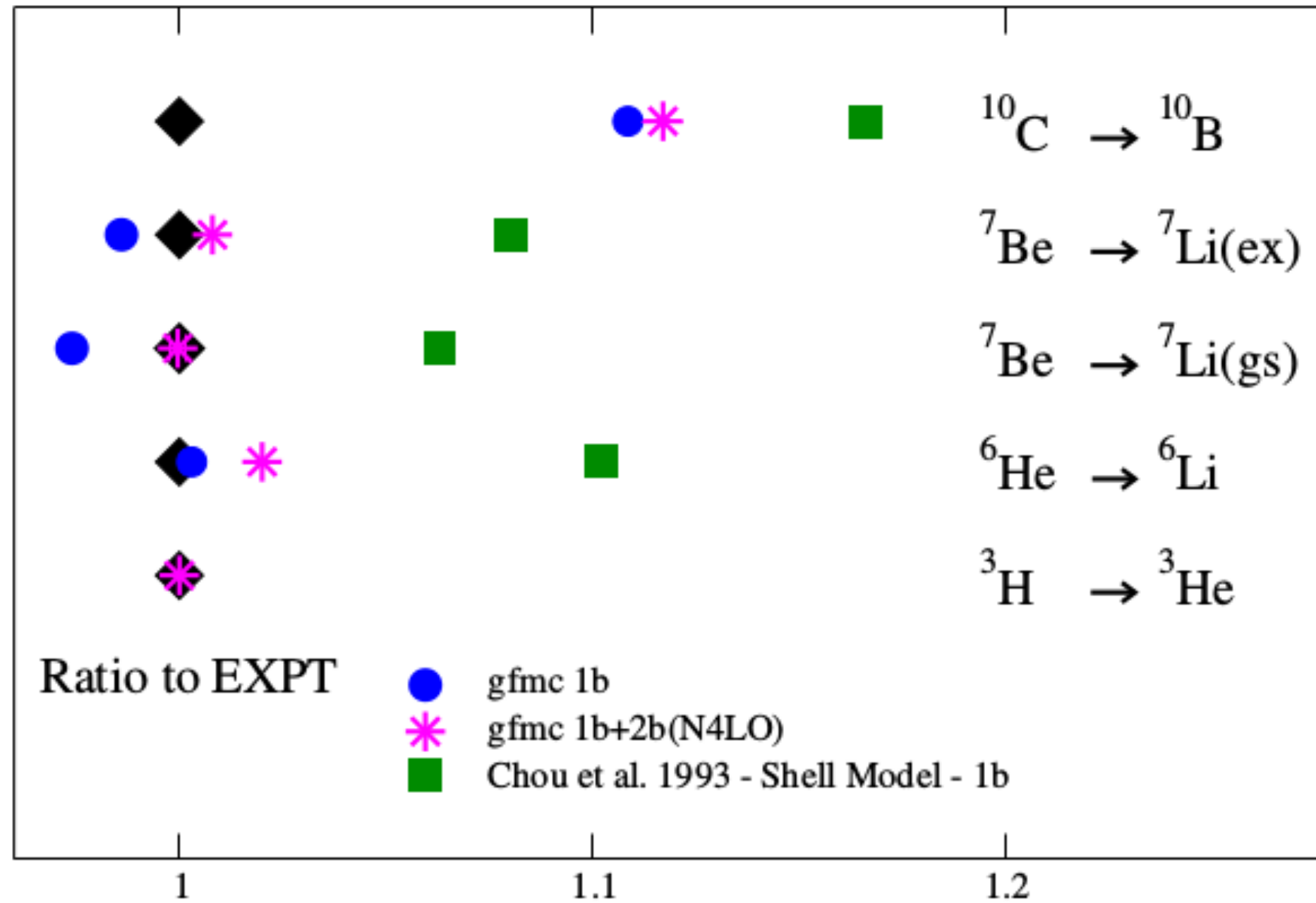
Baroni *et al.* PRC 93, 015501 (2016)

- Beta decay occurs when, in a nucleus with too many protons or too many neutrons, one of the protons or neutrons is transformed into the other.

$$(Z, N) \rightarrow (Z+1, N-1) + e + \bar{\nu}_e$$



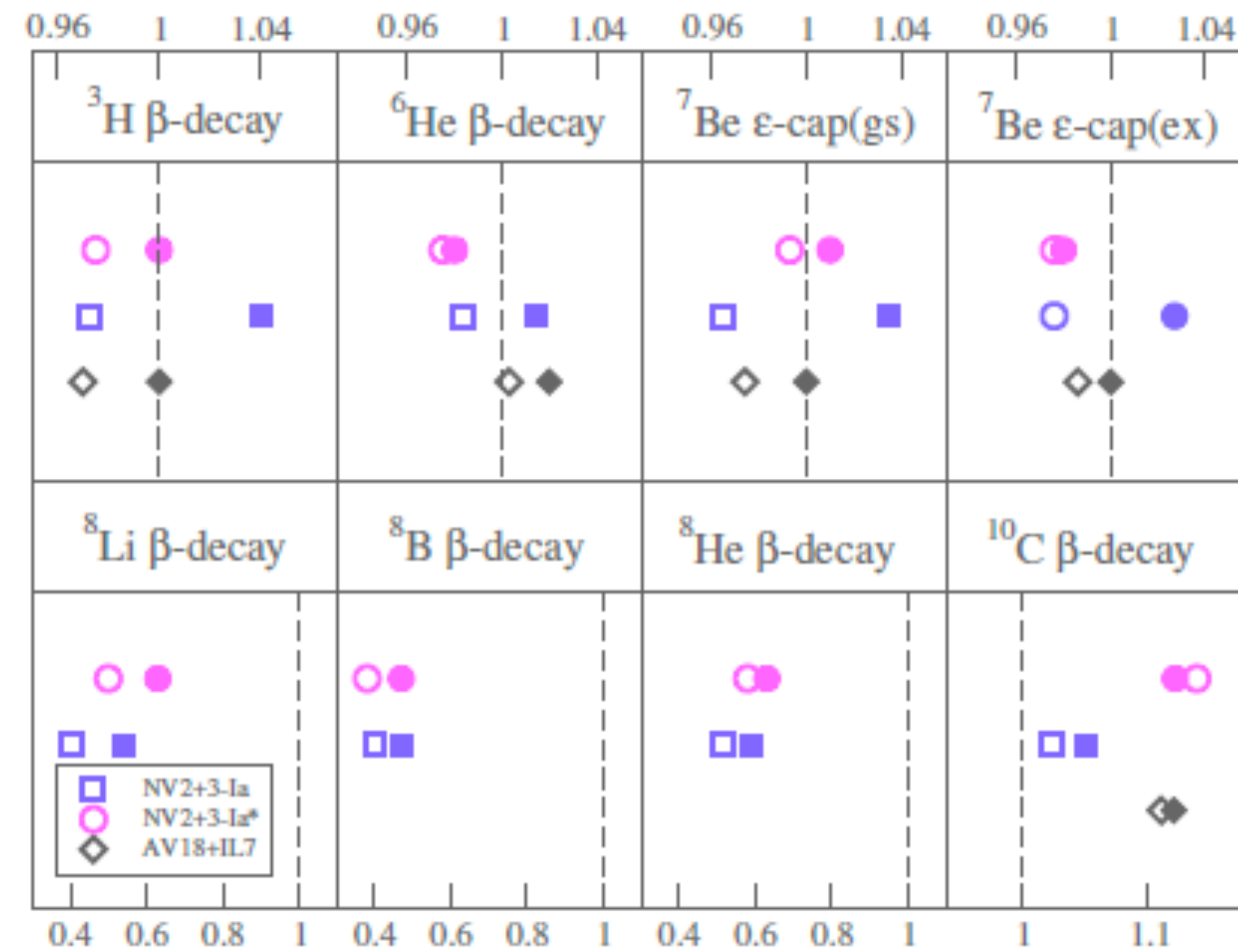
G. King *et al.* PRC 102, 025501 (2020)



gfmc (1b) and gfmc (1b+2b); shell model (1b)

GFMC calculations using AV18/IL7 (rather than chiral) and axial  $\chi$ EFT currents— hybrid calculation

Pastore *et al.* PRC 97 022501 (2018)



GFMC calculations using chiral and axial  $\chi$ EFT currents— consistent calculation

# Neutrinoless Double Beta Decay

In the hypothesis that the  $0\nu\text{DBD}$  is mediated by the exchange of a light neutrino:

$$[T_{1/2}^{0\nu}]^{-1} = G^{0\nu}(Q, Z) |M^{0\nu}|^2 m_{\beta\beta}^2$$

Javier Menendez arXiv:1703.08921 (2017)

## Lepton space-phase integral

- ❖ Depends on the Q-value of the decay and the charge of the final state of the nucleus
- ❖ Can be calculated precisely: for most of the emitters of interest

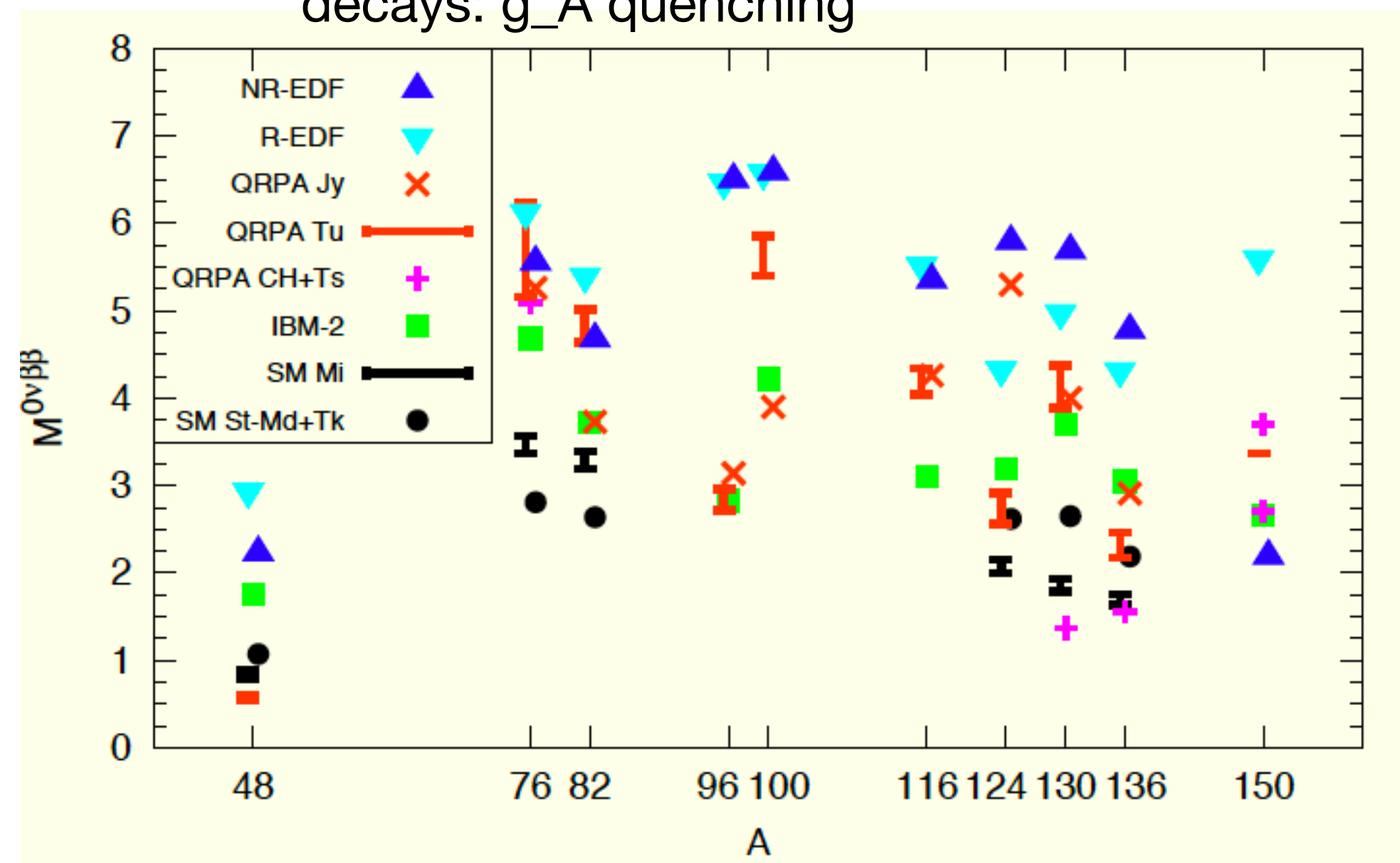
$$10^{-15} - 10^{-16} \text{yr}^{-1}$$

## Nuclear matrix element (NME)

- ❖ Open issues for theorists
- ❖ Spread of about a factor 2-3 in the predicted values for NME for a given isotope
- ❖ Theoretical predictions for these models compared with single beta decays:  $g_A$  quenching

## Effective Majorana mass

- ❖ Depends on combination of neutrino masses and oscillation parameters
- ❖ Uncertainties in the parameters extracted by oscillation experiments and cosmology



# Neutrinoless double-beta decay

- OvDBD: decay mode with the emission of two electrons but without the associated neutrinos:

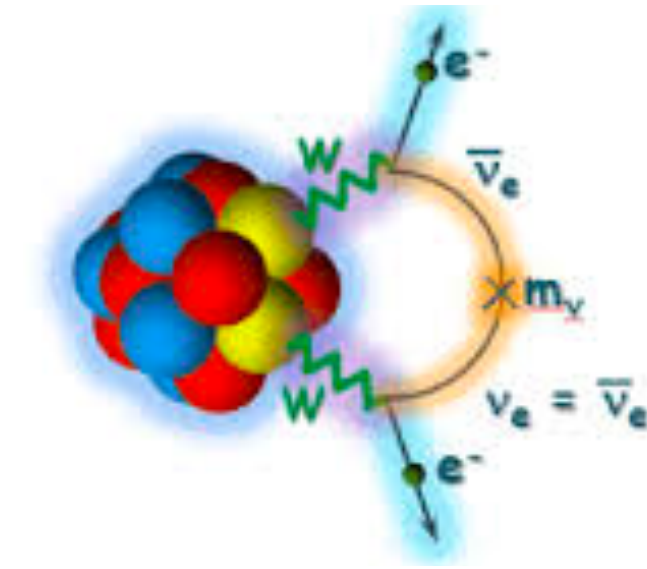
Light-neutrino exchange

Supersymmetric particle exchange

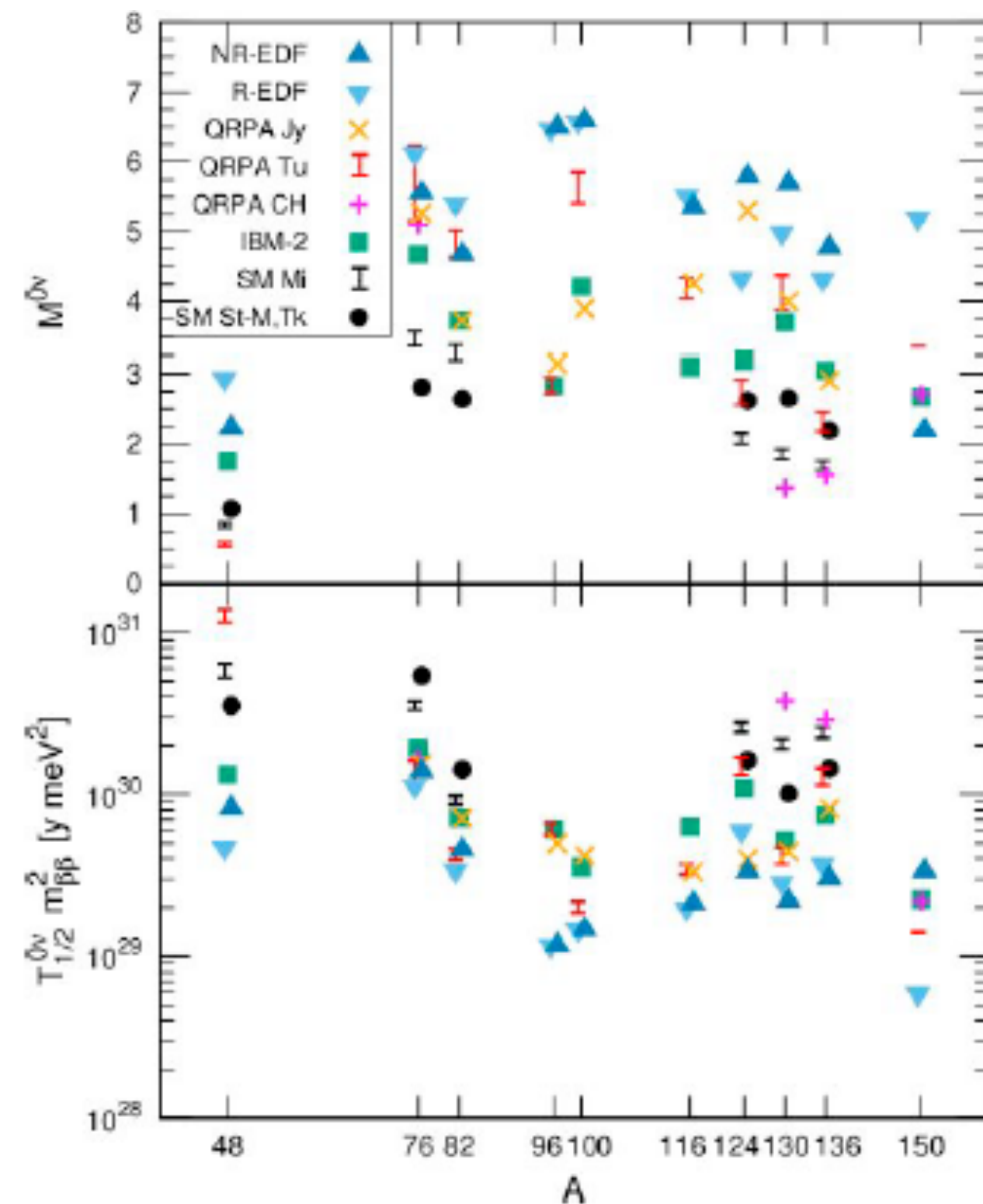
Emission of Majorons (heavy bosons)

.....

- Neutrino physics: Majorana particles
- Lepton number violation
- B-L number violation: relevant to explain asymmetry matter-antimatter



W. Furry, Phys. Rev. 56 1134 (1939).



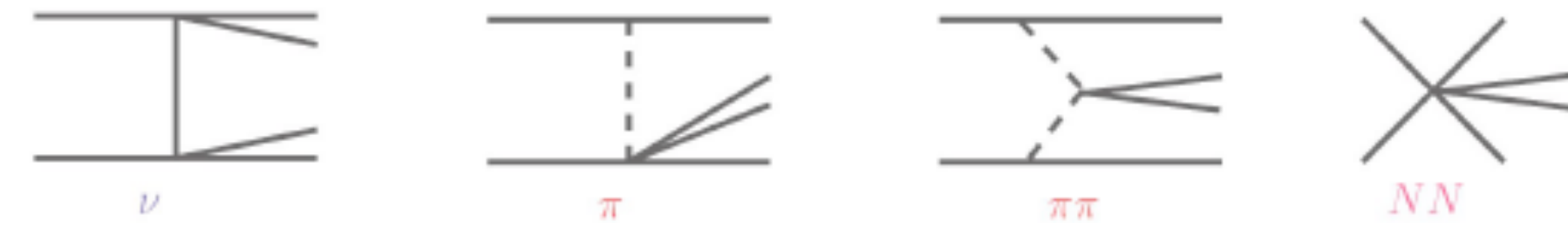
- Matrix elements for nuclei of experimental interest are currently affected by large uncertainties due to truncation in the model space and partial (or missing) inclusion of many-body effects
- We study neutrinoless double beta decay in light nuclei that have been successfully described by ab initio models where correlations and currents can be fully accounted for
- These studies serve as benchmark and to establish the relevance of the various two-body (or more) dynamics inducing the decay

Engel and Menéndez, Rep. Prog. Phys. 80 046301 (2017)



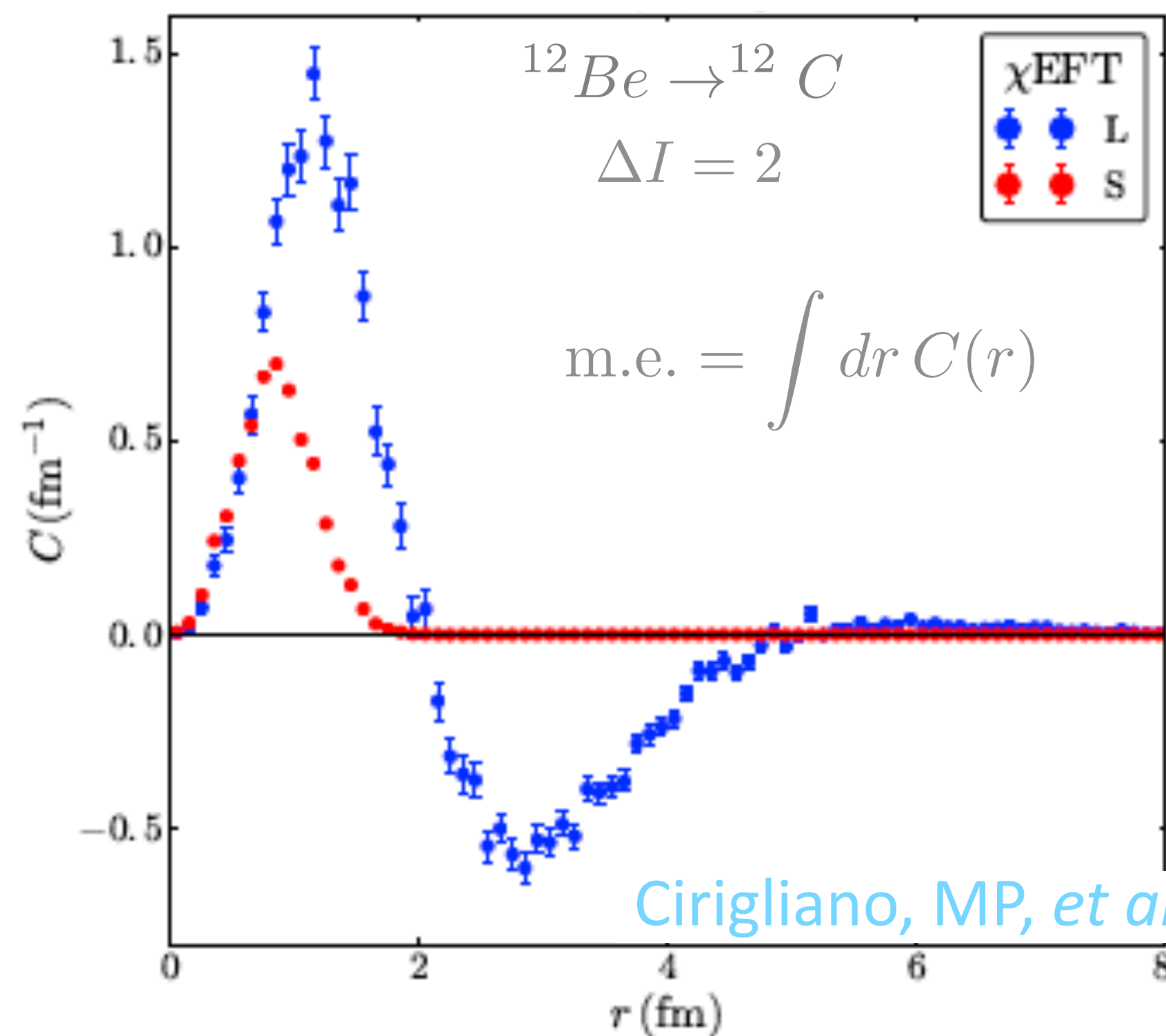
# Neutrinoless double beta matrix elements

- Leading operators in neutrinoless double beta decay are two-body operators
- These observables are particularly sensitive to short-range and two-body physics
- Transition densities calculated in momentum space indicate that the momentum transfer in this process is of the order of  $\sim 200$  MeV



Cirigliano *et al.* PLB769(2017)460, JHEP12(2017)082, PRC97(2018)065501

- Study impact of short-range versus long-range neutrino potential:  $C(r) = C_L(r) + C_S(r)$
- The CIB counter term extracted from potential:  $g_{NN}^\nu = C_{\text{CIB}}$



- $\Delta I=2$  transitions: orthogonal initial and final-state wave functions
- Feature of all isotopes of experimental interest:  $^{48}\text{Ca}$ ,  $^{76}\text{Ge}$ ,  $^{136}\text{Xe}$
- Presence of nodes in the long-range transition densities
- 100% corrections to  $\Delta I=2$  transitions from:  $g_{NN}^\nu$
- If similar in heavier nuclei: large impact on neutrino mass extractions

$A$	Model	$M_F$	$M_{GT}$	$M_T$	$M_L$	$M_S$
6	AV18	1.56	-3.66	0.03	7.45	0.48
	$\chi^{\text{EFT}}$	1.62	-3.85	0.03	7.82	1.15
12	AV18	0.198	-0.349	0.068	0.653	0.518
	$\chi^{\text{EFT}}$	0.223	-0.394	0.083	0.725	0.533

Cirigliano, MP, *et al.* Phys. Rev. C 100, 055504 (2019)

# Partial Muon Capture in Light Nuclei

Weak-interaction Hamiltonian

$$H_W = \frac{G_V}{\sqrt{2}} \int d\mathbf{x} e^{-i\mathbf{k}_\nu \cdot \mathbf{x}} \tilde{l}_\sigma(\mathbf{x}) j^\sigma(\mathbf{x})$$

- Momentum transfer  $q \sim 100 \text{ MeV}$
- Validation of vector and axial charges and currents
- For light nuclei, you can approximate the muon as at rest in a Hydrogen-like 1s orbital

$$\begin{aligned} \Gamma = & \frac{G_V^2}{2\pi} \frac{|\psi_{1s}^{\text{av}}|^2}{(2J_i + 1) \text{recoil}} \frac{E_\nu^{*2}}{\sum_{M_f, M_i}} \left[ |\langle J_f, M_f | \rho(E_\nu^* \hat{\mathbf{z}}) | J_i, M_i \rangle|^2 + |\langle J_f, M_f | \mathbf{j}_z(E_\nu^* \hat{\mathbf{z}}) | J_i, M_i \rangle|^2 \right. \\ & + 2 \text{Re} \left[ \langle J_f, M_f | \rho(E_\nu^* \hat{\mathbf{z}}) | J_i, M_i \rangle \langle J_f, M_f | \mathbf{j}_z(E_\nu^* \hat{\mathbf{z}}) | J_i, M_i \rangle^* \right] + |\langle J_f, M_f | \mathbf{j}_x(E_\nu^* \hat{\mathbf{z}}) | J_i, M_i \rangle|^2 \\ & \left. + |\langle J_f, M_f | \mathbf{j}_y(E_\nu^* \hat{\mathbf{z}}) | J_i, M_i \rangle|^2 - 2 \text{Im} \left[ \langle J_f, M_f | \mathbf{j}_x(E_\nu^* \hat{\mathbf{z}}) | J_i, M_i \rangle \langle J_f, M_f | \mathbf{j}_y(E_\nu^* \hat{\mathbf{z}}) | J_i, M_i \rangle^* \right] \right] \end{aligned}$$

# Partial Muon Capture Rates with QMC: ${}^3\text{He}(\mu^-, \nu_\mu){}^3\text{H}$

Momentum transfer  $q \sim 100$  MeV

- QMC rate for  ${}^3\text{He}(1/2^+; 1/2) \rightarrow {}^3\text{H}(1/2^+; 1/2)$

- ▶  $\Gamma_{\text{VMC}} = 1512 \text{ s}^{-1} \pm 32 \text{ s}^{-1}$
- ▶  $\Gamma_{\text{GFMC}} = 1476 \text{ s}^{-1} \pm 43 \text{ s}^{-1}$
- ▶  $\Gamma_{\text{expt}} = 1496.0 \text{ s}^{-1} \pm 4.0 \text{ s}^{-1}$

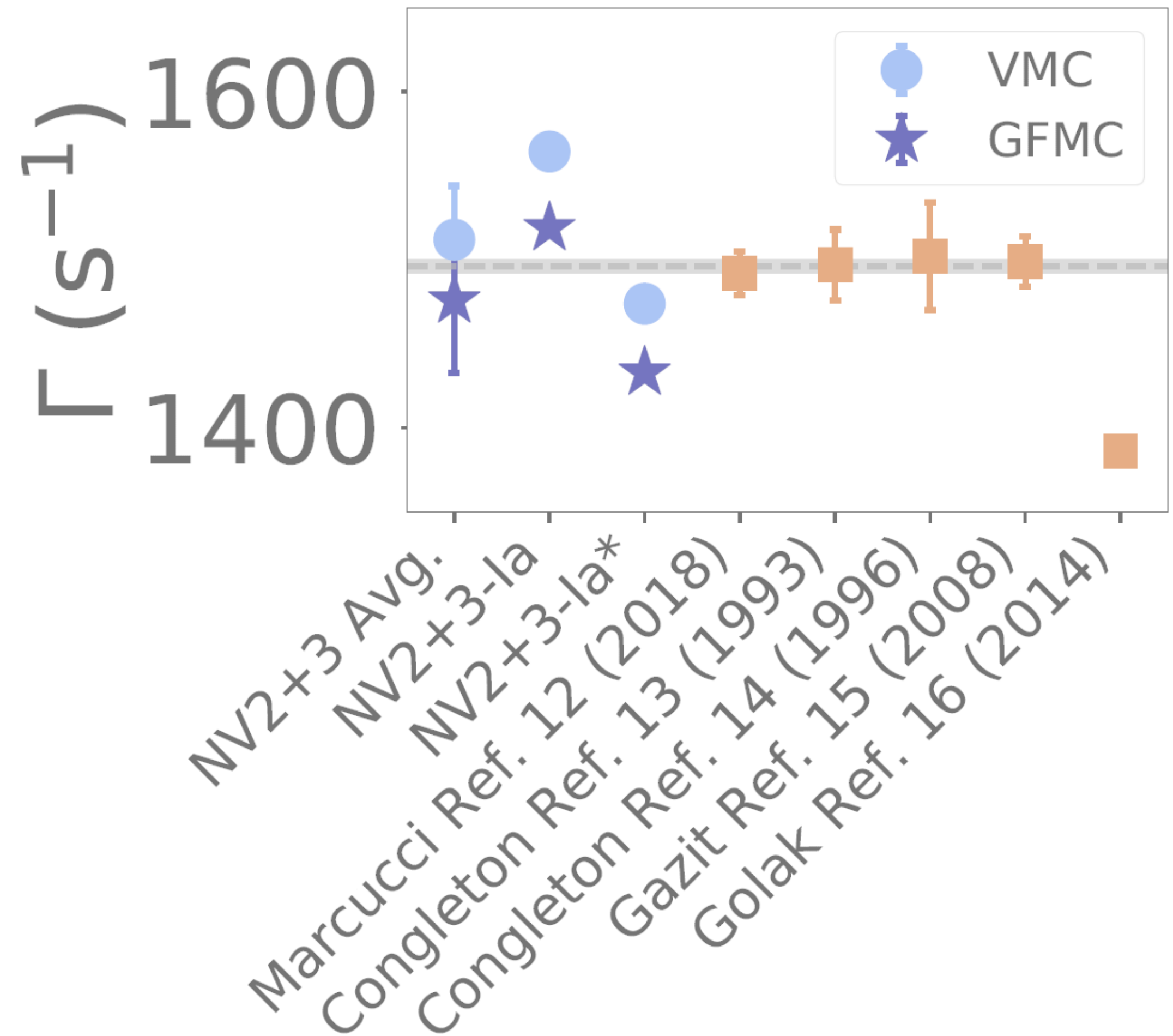
[Ackerbauer et al. Phys. Lett. B417 (1998)]

- The inclusion of 2b electroweak currents increase the rate by about 9% to 16%.

- uncertainty estimates:

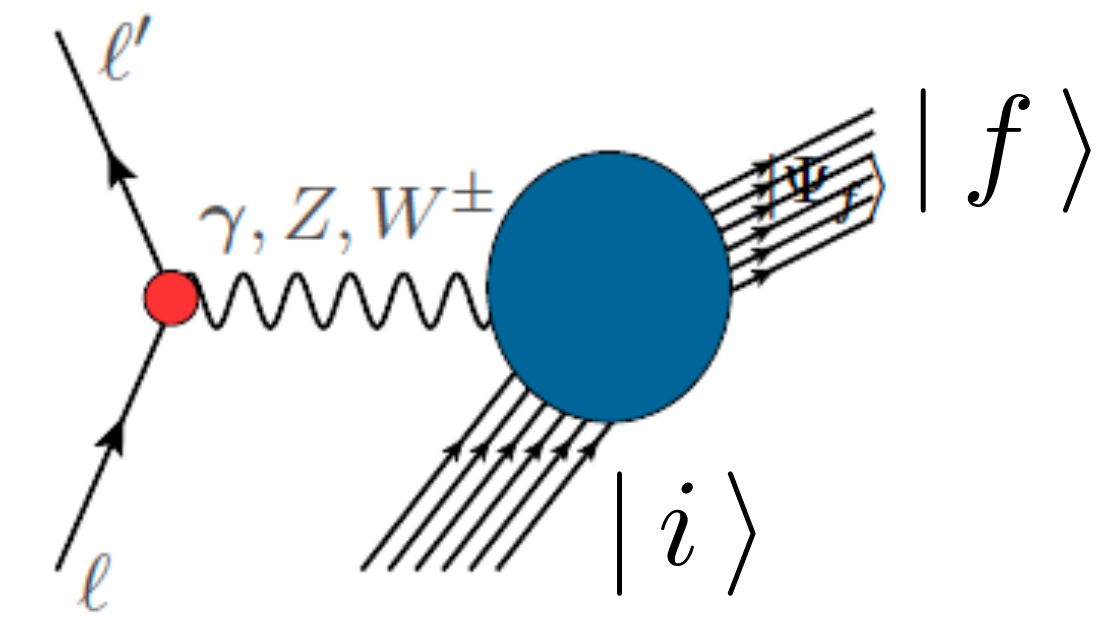
- Cutoff:  $8 \text{ s}^{-1}$  (0.5%)
- Energy range of fit:  $11 \text{ s}^{-1}$  (0.7%)
- Three-body fit:  $27 \text{ s}^{-1}$  (1.8%)
- Systematic:  $9 \text{ s}^{-1}$  (0.6%)

King et al. PRC 105 (2022) 4, L042501





# Lepton-Nucleus Scattering: Inclusive Processes



- Inclusive lepton scattering off a the nucleus: five response functions

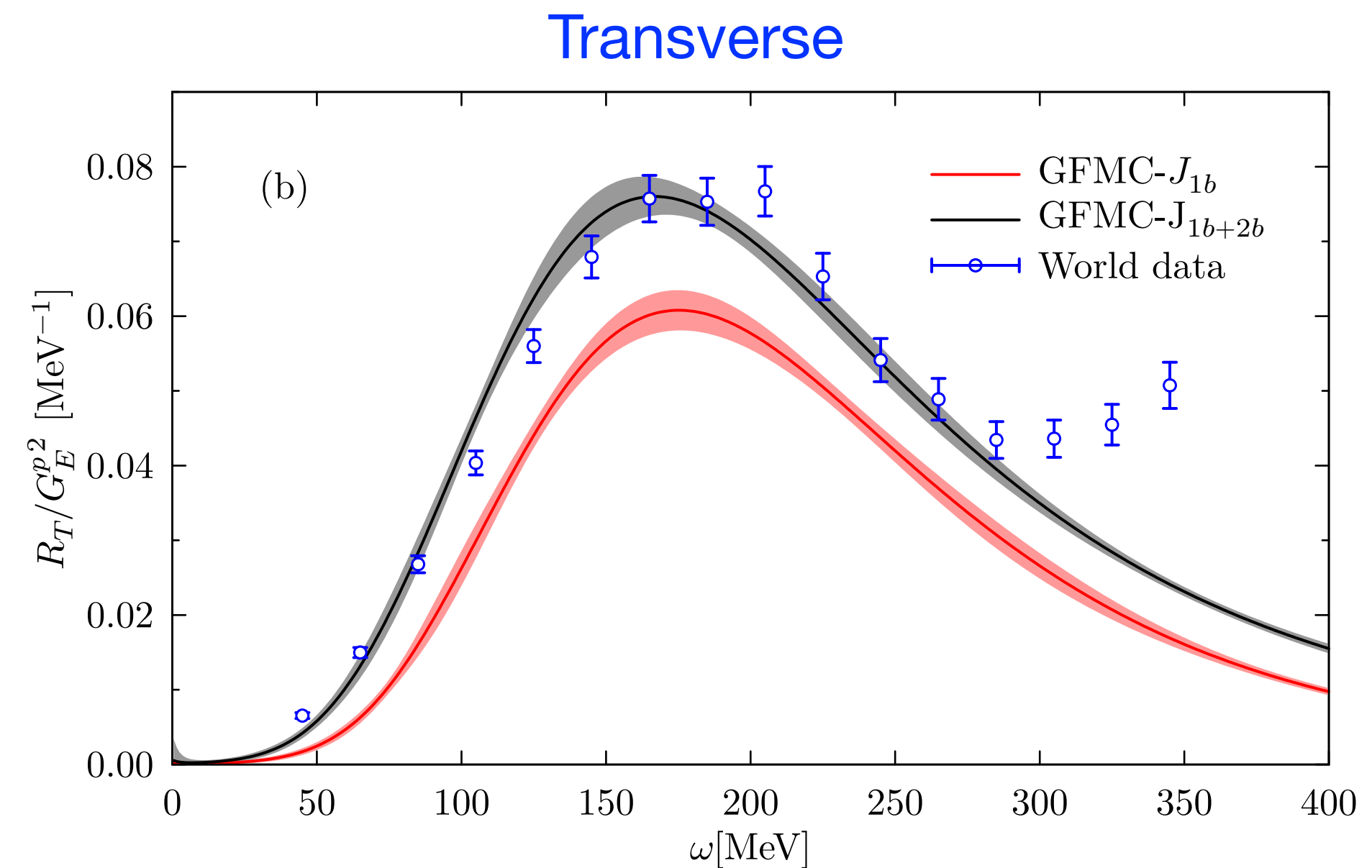
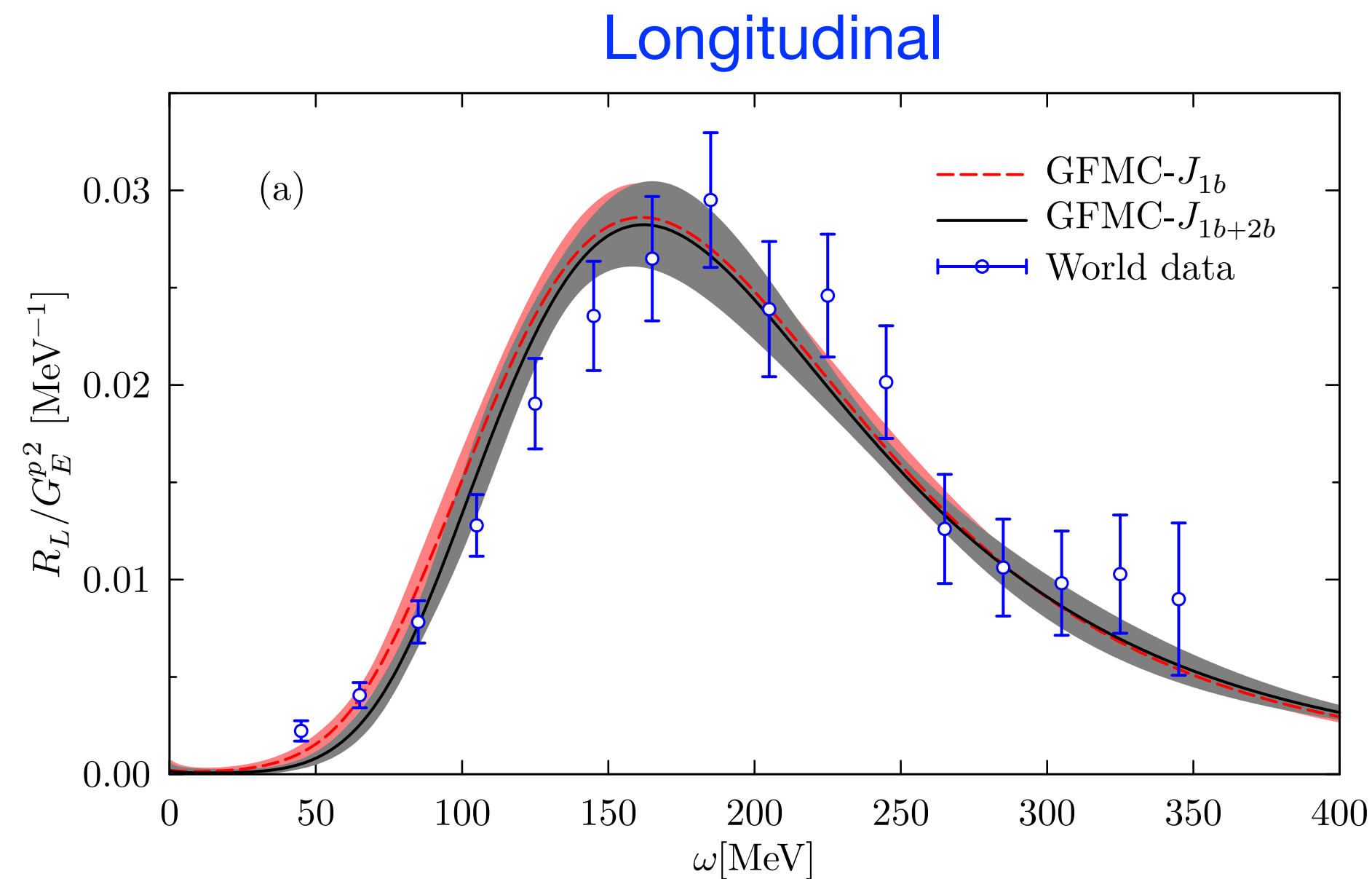
$$\frac{d\sigma}{d\epsilon'_l d\Omega_l} \propto \left[ v_{00} R_{00} + v_{zz} R_{zz} - v_{0z} R_{0z} + v_{xx} R_{xx} \mp v_{xy} R_{xy} \right]$$

- For the EM case only two response functions survive: longitudinal  $R_{00}$  and transverse  $R_{xx}$  which are obtained from the charge and transverse current operators  $R_\alpha(q, \omega) = \sum_f \delta(\omega + E_0 - E_f) |\langle f | O_\alpha(\mathbf{q}) | 0 \rangle|^2$   $O_L = \rho$   
 $O_T = \mathbf{j}$

Euclidean response: GFMC calculations

$$\int_0^\infty d\omega e^{-\tau\omega} R_{\alpha\beta}(q, \omega) = \langle i | j_\alpha^\dagger(\mathbf{q}) e^{-\tau(H-E_i)} j_\beta(\mathbf{q}) | i \rangle$$

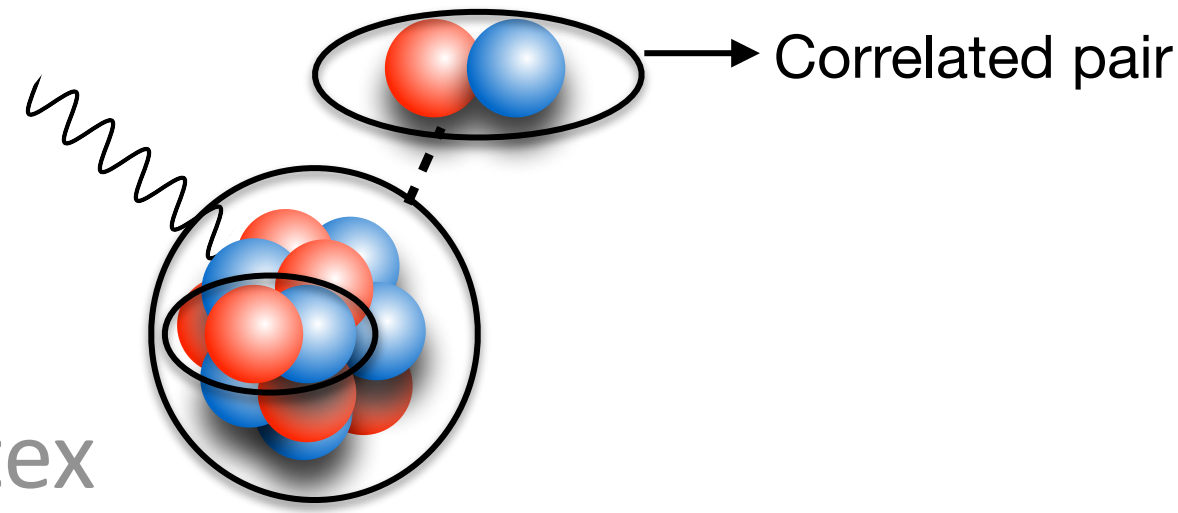
Inversion back to obtain the response by maximum entropy methods



# Lepton-Nucleus Scattering: Exclusive Processes

## Short-Time-Approximation:

- Based on factorization
- Response functions are given by the scattering from pairs of fully interacting nucleons that propagate into a correlated pair of nucleons
- Allows to retain both two-body correlations and currents at the vertex
- Describe electroweak scattering for  $A > 12$  without losing two-body physics
- Incorporate relativistic effects
- Provides “more” exclusive information in terms of nucleon-pair kinematics via the Response Densities



Response **Functions**: integral over real time

$$R_{\alpha\beta}(\omega, \mathbf{q}) = \int \frac{dt}{2\pi} e^{i(\omega + E_0)t} \langle 0 | J_{\alpha}^{\dagger}(\mathbf{q}) e^{-iHt} J_{\beta}(\mathbf{q}) | 0 \rangle$$

The two main assumption underlying the STA are:

1. Only the one- and two-body terms are kept in the current-current correlator

$$j^{\dagger}(i) e^{-iHt} j(i) + j^{\dagger}(i) e^{-iHt} j(j) + j^{\dagger}(i) e^{-iHt} j(ij) + j^{\dagger}(ij) e^{-iHt} j(ij)$$

2. In the particle propagator the Hamiltonian is rewritten as

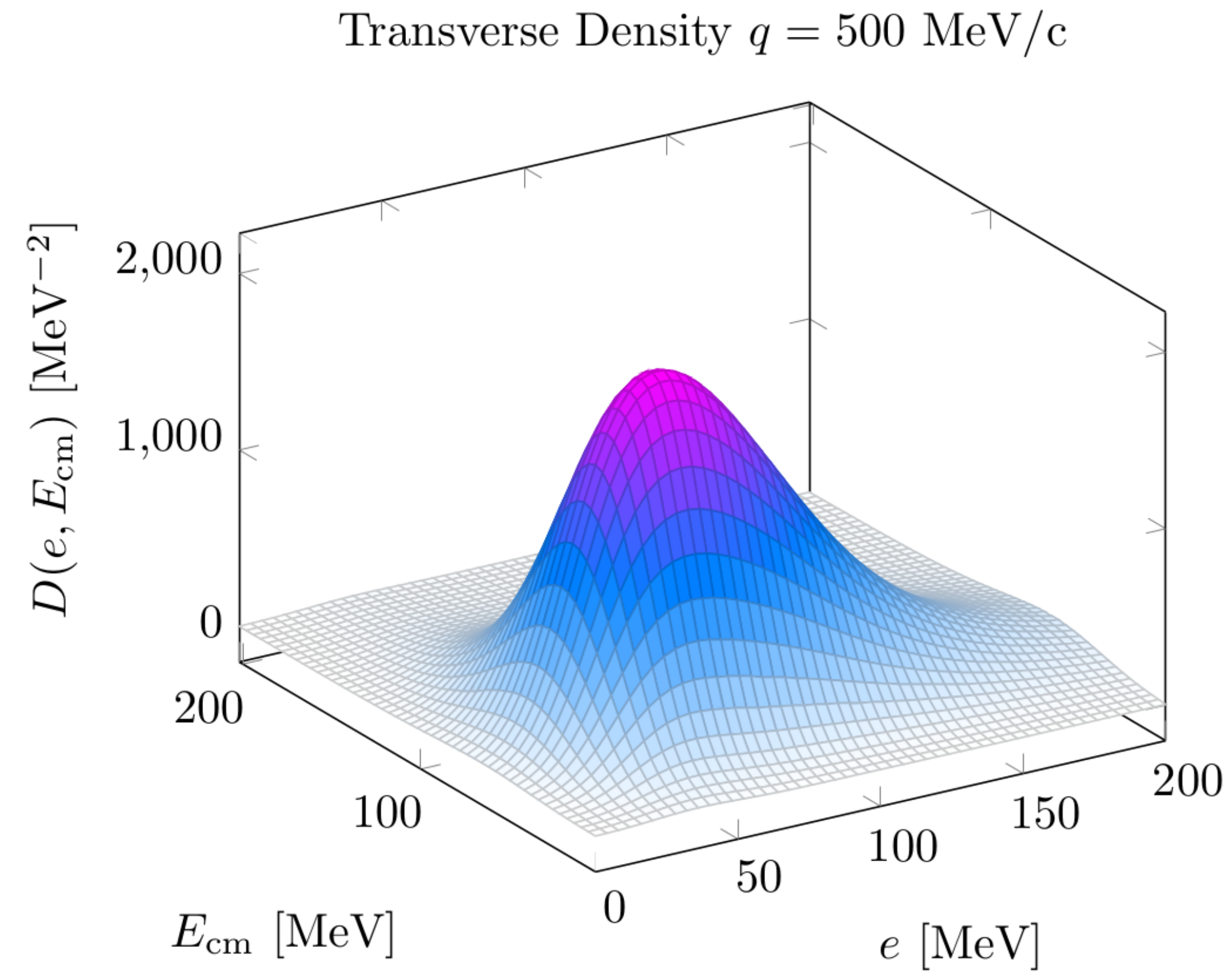
$$H = \sum_i \frac{p_i^2}{2m} + \sum_{ij} v_{ij}$$

Response **Densities**:

$$R(q, \omega) = \int_0^{\infty} de dE_{\text{cm}} \delta(\omega + E_0 - e - E_{\text{cm}}) D(e, E_{\text{cm}})$$

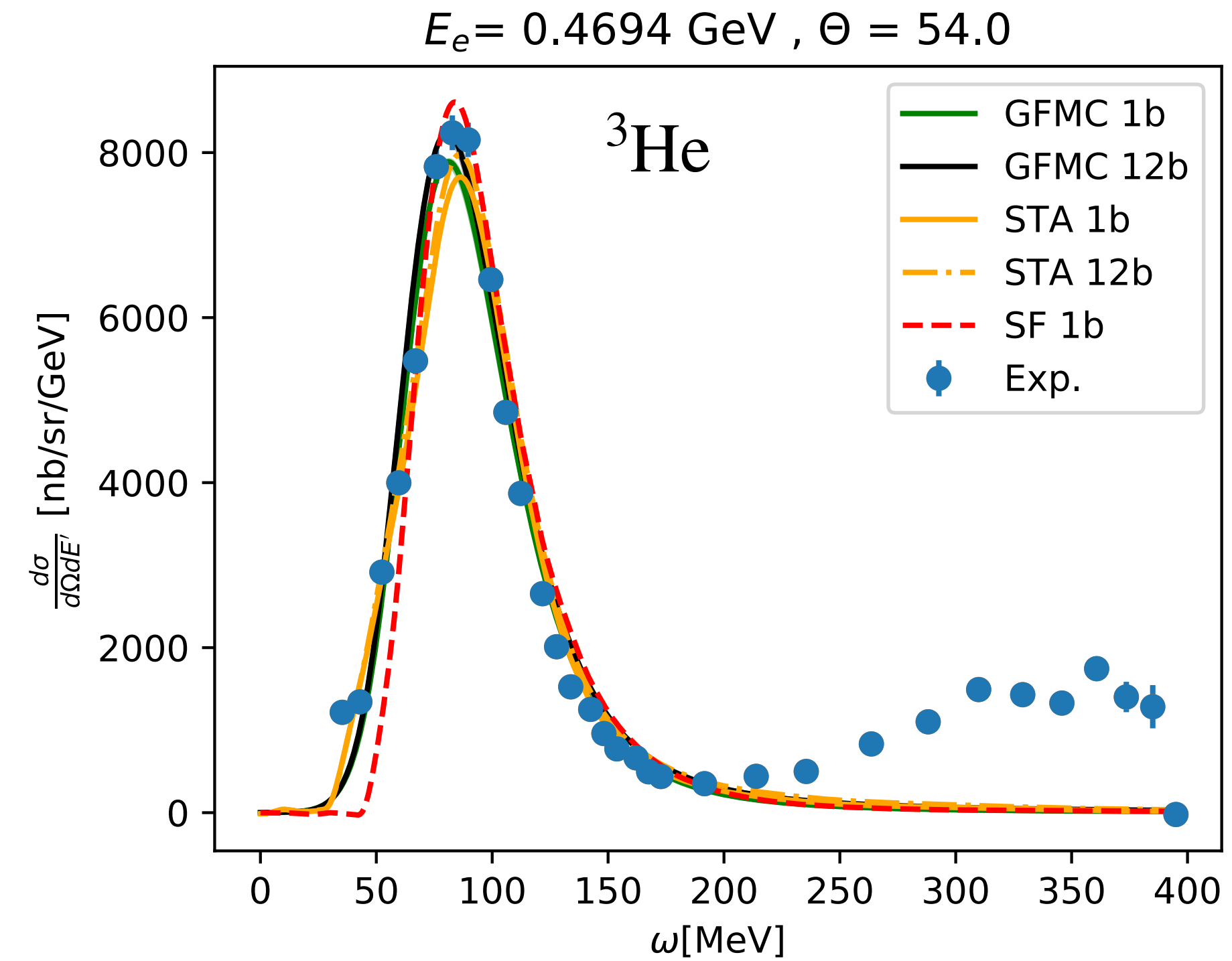
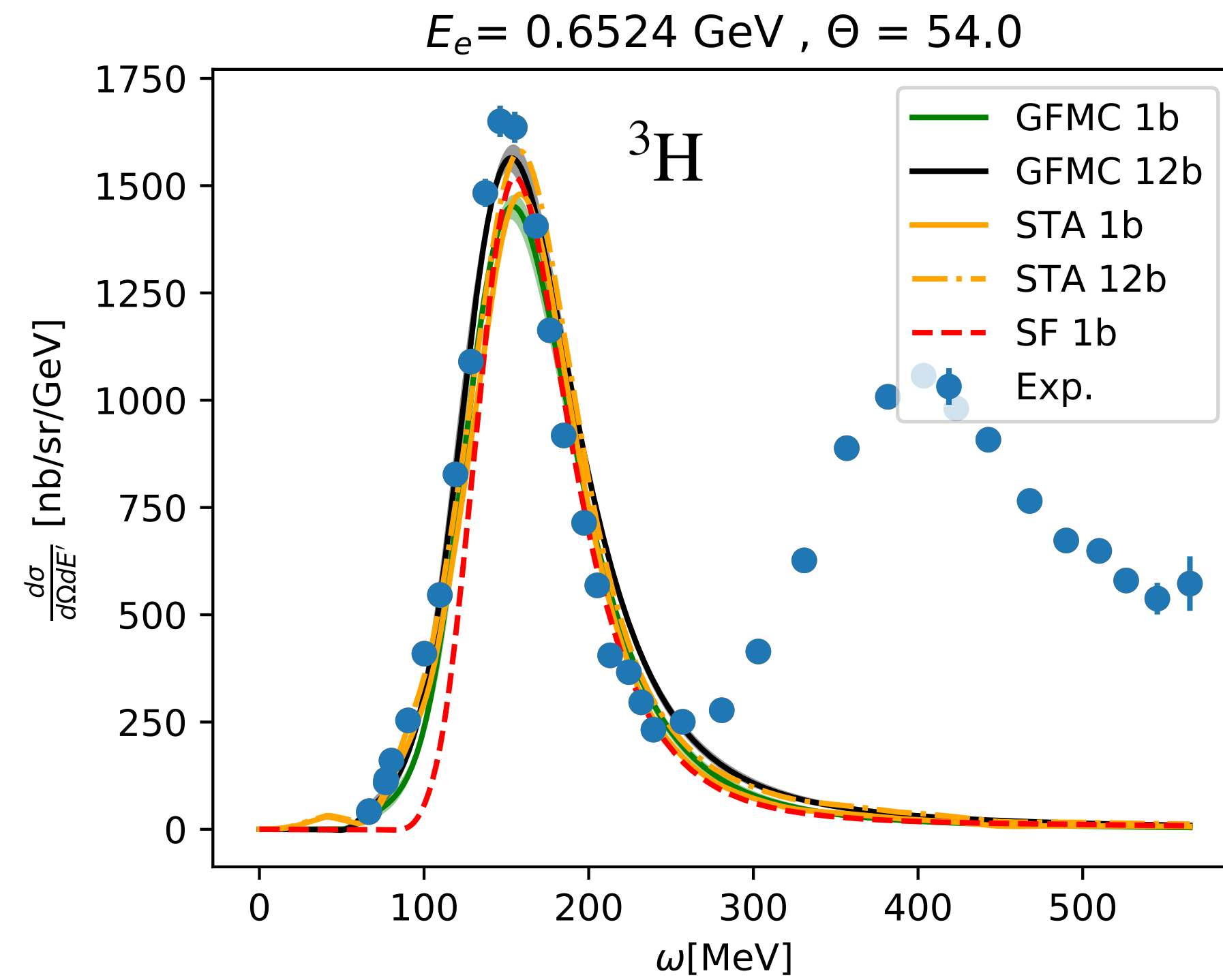
$E_{\text{cm}}$  and  $e$  are the CM and relative energy of the struck nucleon pair

# Transverse Response Density: $e^{-4}\text{He}$ scattering



Pastore *et al.* PRC101(2020)044612

# Cross sections $^3\text{H}$ and $^3\text{He}$ : benchmark between GFMC and STA

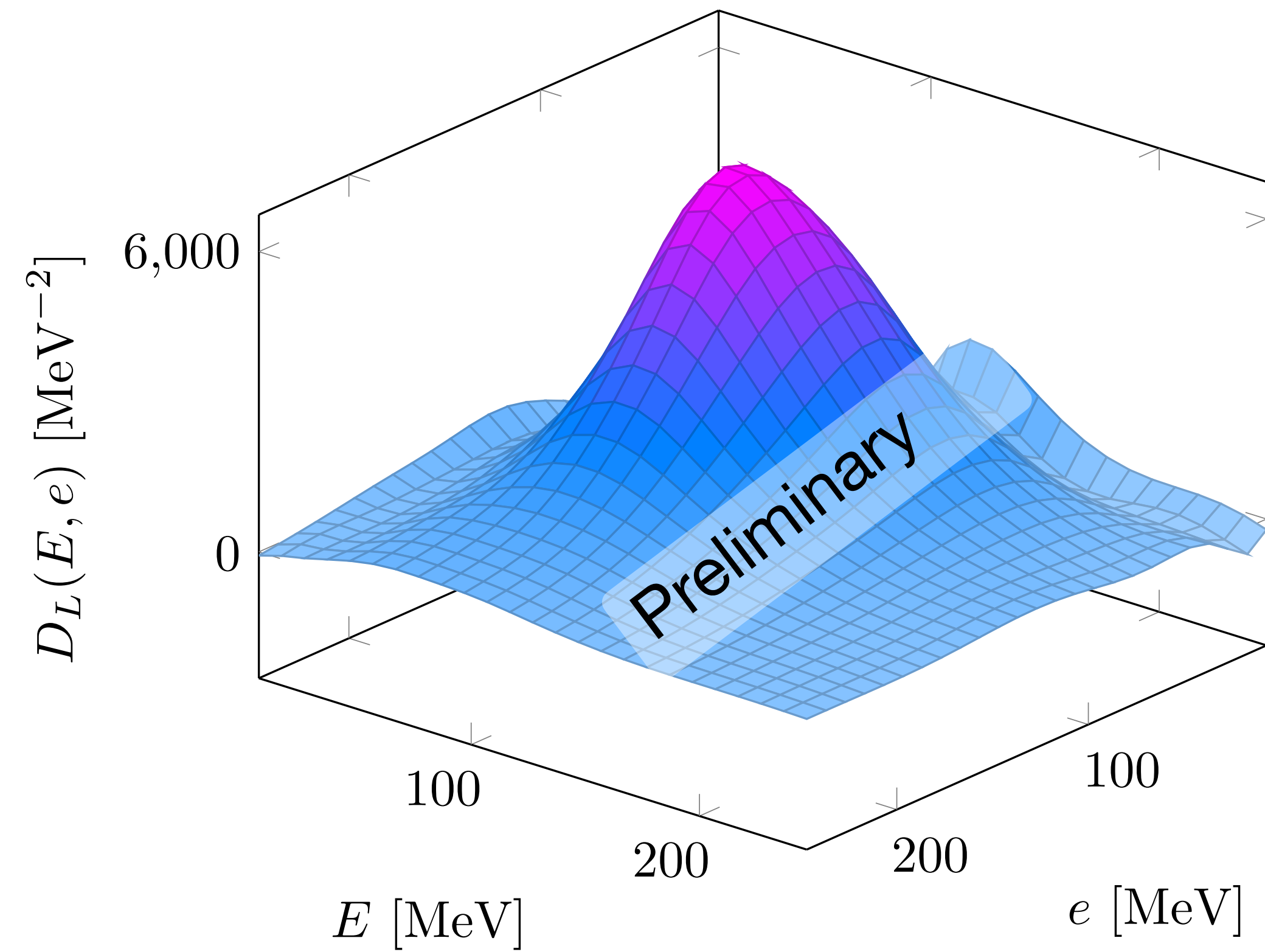


Andreoli et al. Phys. Rev. C 105, 014002

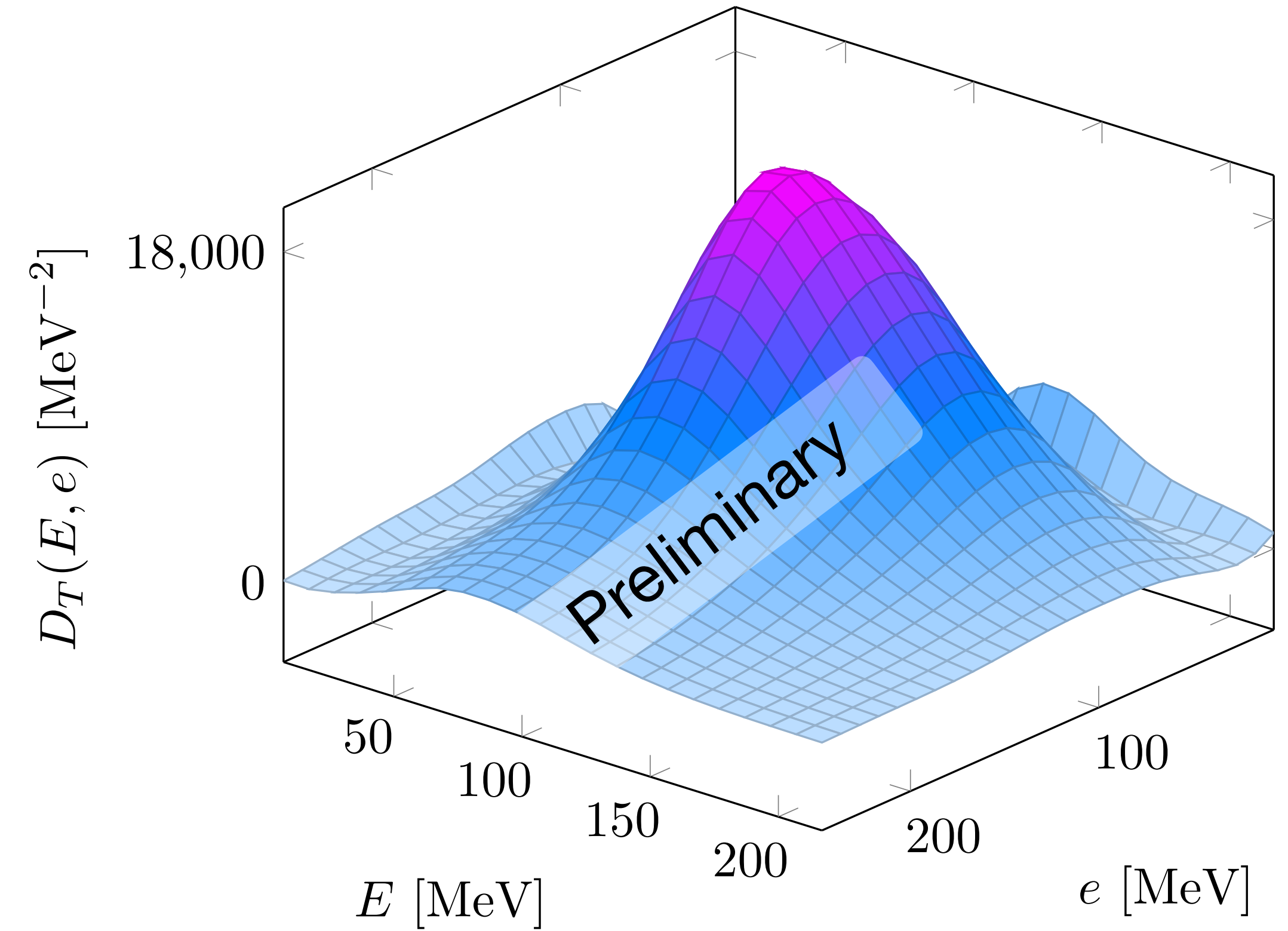


# Response densities for $^{12}\text{C}$

Longitudinal Density  $q = 570$  MeV



Transverse Density  $q = 570$  MeV

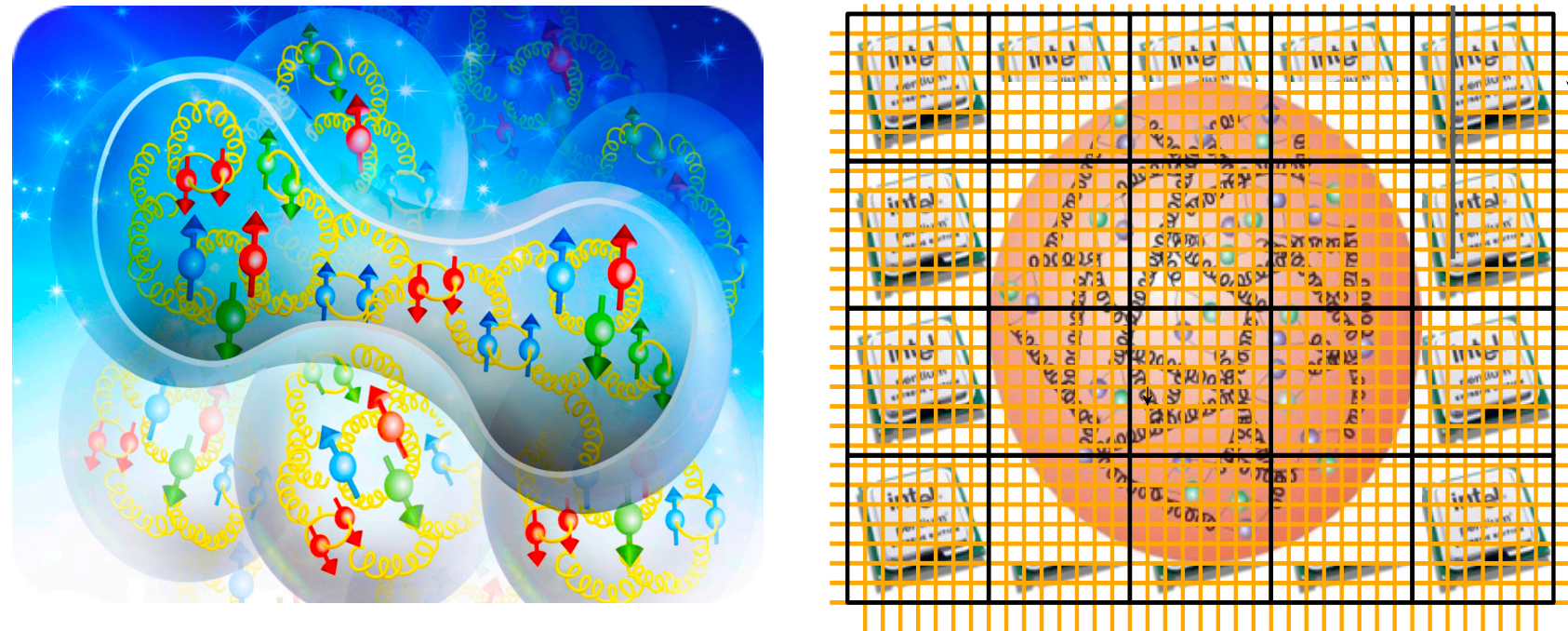


Preliminary results for longitudinal and transverse response densities in  $^{12}\text{C}$

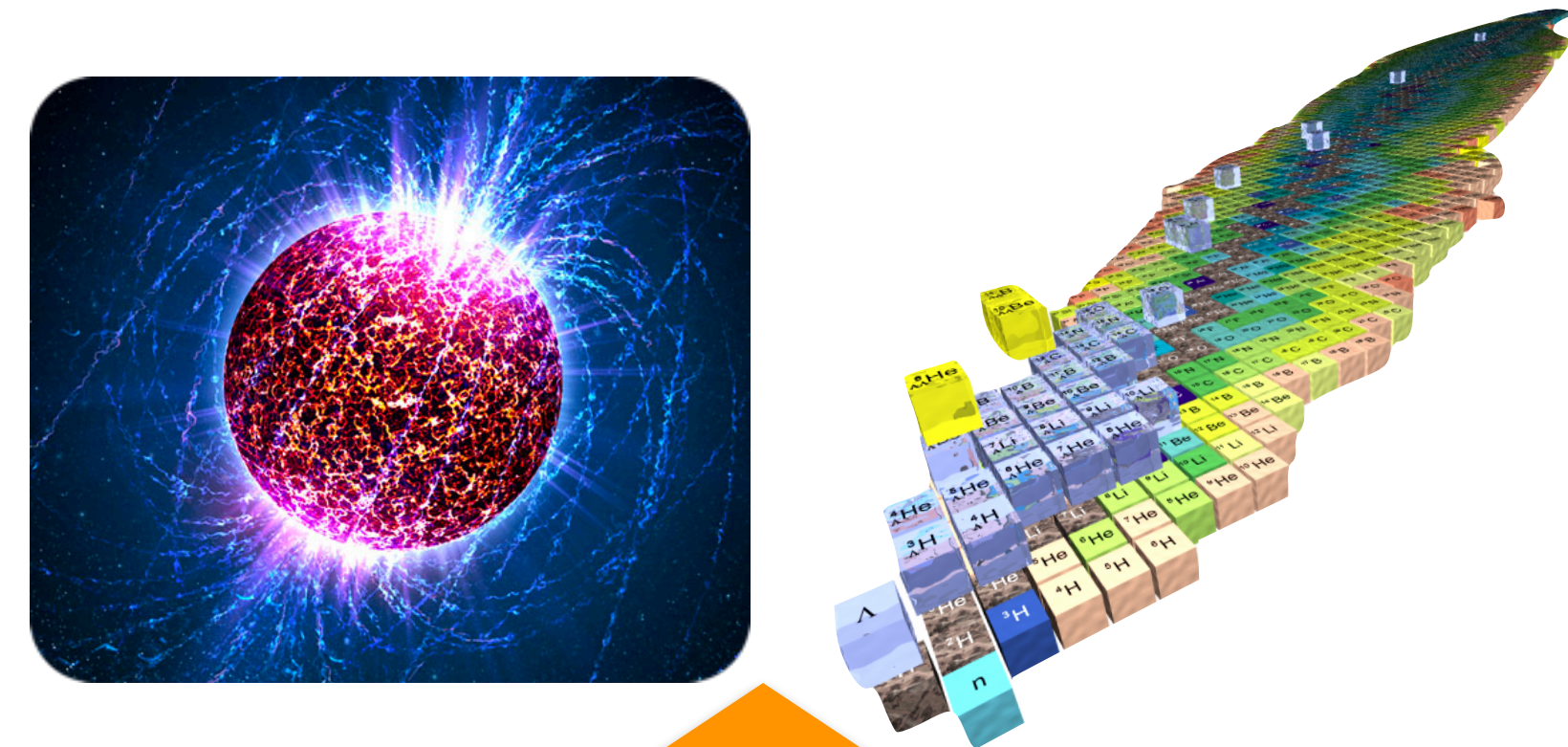


# Summary: Workflow for the microscopic model nuclear theory

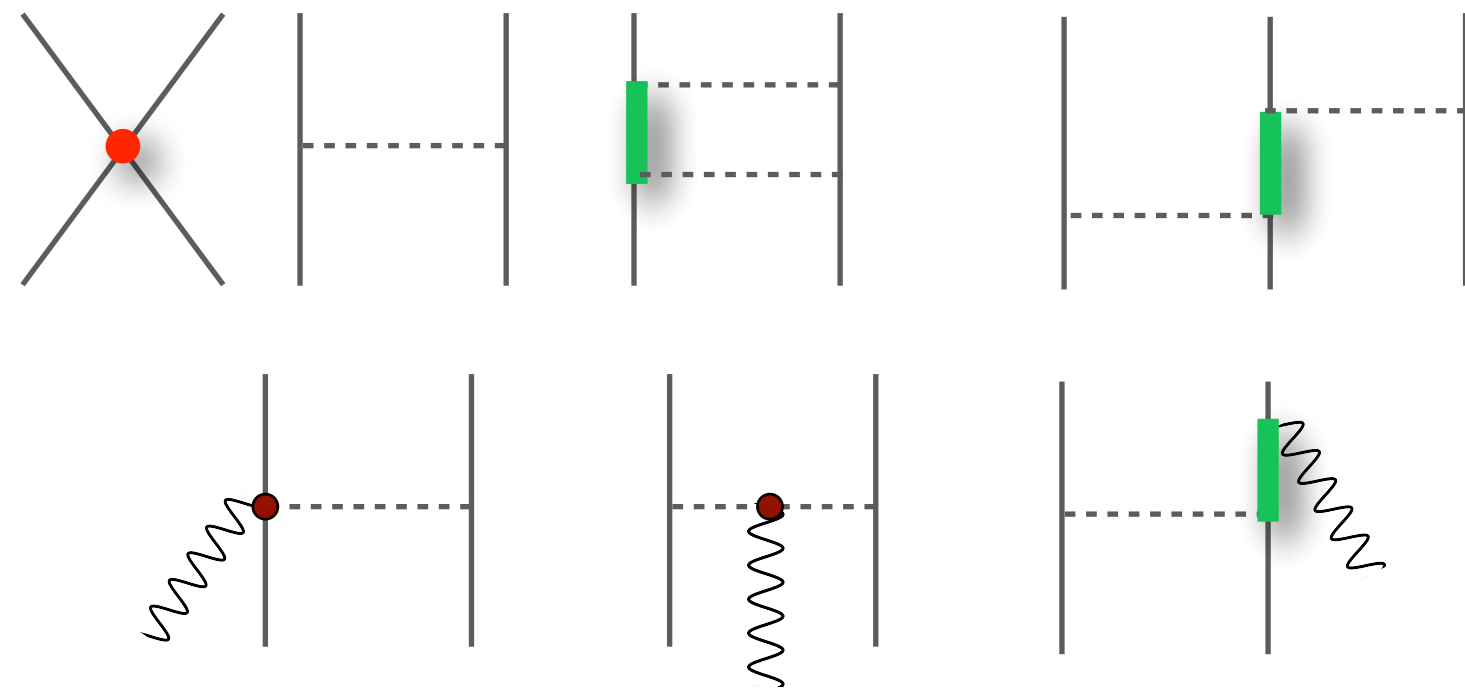
## Quantum Chromodynamics



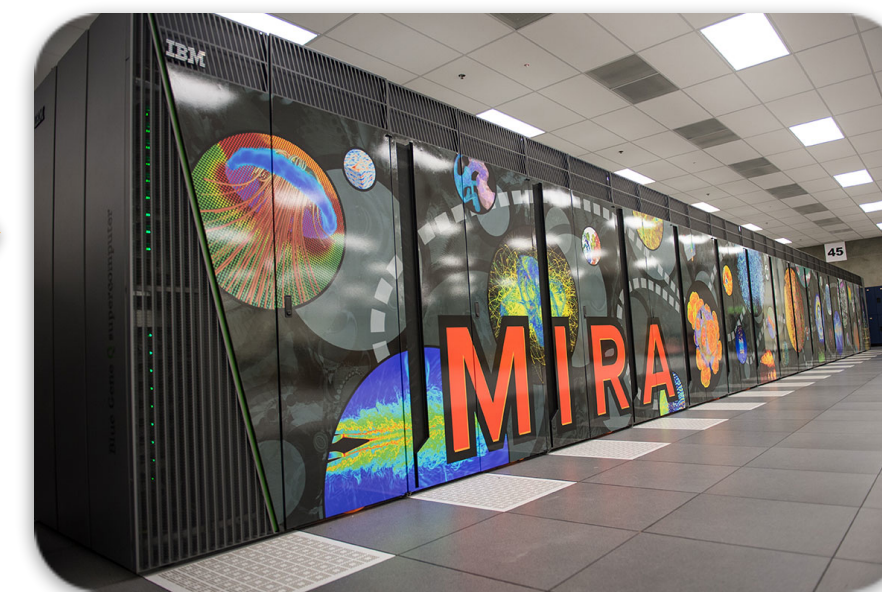
## Atomic nuclei and nucleonic matter



## Hamiltonian and electroweak currents



## Accurate nuclear many-body methods



$$H|\Psi_n\rangle = E_n|\Psi_n\rangle$$

$$J_{mn} = \langle\Psi_m|J|\Psi_n\rangle$$

**THANK YOU!!!**